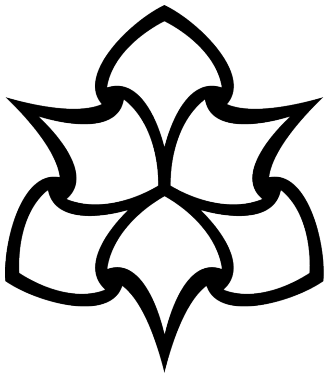

First posted online on 27 January 2020 as 10.1242/jeb.217117
Access the most recent version at http://jeb.biologists.org/lookup/doi/10.1242/jeb.217117

The impact of a high-fat diet in mice is dependent on duration and age, and differs between muscles

Messa GAM[a], Piasecki M[b], Hurst J[c], Hill C[c,d], Tallis J[c], Degens H[a,e,f]

[a] Department of Life Sciences, Research Centre for Musculoskeletal Science & Sports Medicine, Manchester Metropolitan University, UK

[b] Clinical, Metabolic and Molecular Physiology, MRC-ARUK Centre for Musculoskeletal Ageing Research and National Institute for Health Research (NIHR) Nottingham Biomedical Research Centre, University of Nottingham, UK

[c] Center for Sport, Exercise and Life Sciences, Alison Gingell Building, Coventry University, Priory Street, Coventry CV1 5FB, UK

[d] Randall Centre for Cell and Molecular Biophysics, New Hunt's House, Guy's Campus, Kings College, London, UK

[e] Institute of Sport Science and Innovations, Lithuanian Sports University, Lithuania

[f] University of Medicine and Pharmacy of Targu Mures

Address for correspondence:

Prof Hans Degens

School of Healthcare Science

Manchester Metropolitan University

John Dalton Building; Chester Street

Manchester M1 5GD

United Kingdom

Phone: +44.161.247.5686

E-mail: h.degens@mmu.ac.uk

Abstract

Prolonged high-fat diets (HFD) can cause intramyocellular lipids (IMCL) accumulation that may negatively affect muscle function. We investigated the duration of a HFD required to instigate these changes, and whether effects are muscle-specific and aggravated in older age. Muscle morphology was determined in the soleus, extensor digitorum longus (EDL) and diaphragm muscles from female CD-1 mice divided into 5 groups: young fed a HFD for 8 weeks (YS-HFD, n = 16), young fed a HFD for 16 weeks (YL-HFD, n = 28) and young control (Y-CON, n = 28). The young animals were 20 weeks old at the end of the experiment. Sixty 70-week-old female CD-1 mice received either a normal diet (O-CON, n = 30) or a HFD for 9 weeks (OS-HFD, n = 30). Body mass, body mass index and IMCL content increased in old OS-HFD ($p \leq 0.003$). In the young mice, this increase was seen in YL-HFD and not YS-HFD ($p \leq 0.006$). The soleus and diaphragm fibre cross-sectional area (FCSA) in YL-HFD was larger compared to Y-CON ($p \leq 0.004$) while old mice had a larger soleus FCSA compared to CON after only 9 weeks on a HFD ($p < 0.001$). The FCSA of the EDL muscle did not differ significantly between groups. Oxidative capacity of fibres increased in young only, irrespective of HFD duration ($p < 0.001$). High-fat diet-induced morphological changes occur earlier in the old animals when compared to young, and adaptations to HFD are muscle-specific with the EDL being least responsive.

Keywords: capillarization, capillary domains, diaphragm, high-fat diet, soleus

Introduction

More than 1.9 billion adults (approximately 24.6% of the world's population) over the age of 18 are overweight or obese (WHO, 2018). Under obesogenic conditions, such as excessive and prolonged consumption of high-fat diets (HFD), energy intake exceeds expenditure, causing an accumulation of lipids in adipose tissues and ectopically in non-adipose tissues, including skeletal muscle where excess lipids are stored as intramyocellular lipids (IMCL; lipid *within* the muscle fiber) (Addison et al., 2014; Unger et al., 2010). In addition to negative effects of systemic inflammation and insulin resistance associated with obesity (Cesari et al., 2005) on myogenesis and muscle function, muscular lipid accumulation itself can also compromise excitation-contraction coupling, metabolism and contractile function of skeletal muscle (Bonen et al., 2015; Choi et al., 2016; Hancock et al., 2008; Montgomery et al., 2017; Tallis et al., 2018).

The prevalence of sarcopenic obesity, the presence of sarcopenia and obesity in an individual, is increasing in the Western world (Batsis and Villareal, 2018). While the absolute strength and mass of postural and locomotor muscles may be larger in obese than non-obese individuals (Abdelmoula et al., 2012; Maffiuletti et al., 2007; Tomlinson et al., 2014), probably due to the higher load on the postural muscles during standing and locomotion (Garcia-Vicencio et al., 2016), muscle strength normalized to body mass is lower in obese than non-obese adolescents (Lee et al., 2012), young (Maffiuletti et al., 2007) and old adults (Tomlinson et al., 2014; Zoico et al., 2004). In addition, the specific tension (force per cross-sectional area) may also be lower in obesity, as seen in *in vitro* rodent studies (Hurst et al., 2019; Tallis et al., 2017b) and in human studies (Erskine et al., 2017). In addition, it has been reported that the age-related loss of muscle strength is larger in obese than non-obese women (Tomlinson et al., 2014).

The effects of obesity on skeletal muscle are not systemic as reflected by the different response in locomotory and respiratory muscles (Tallis et al., 2018). In a study on obese men and women, the predominant upper-body fat distribution was not associated with a significant impairment of respiratory muscle strength (Magnani and Cataneo, 2007). In the lower leg, however, muscle strength is at least partly attributable to a lower specific tension (maximal muscle force per cross-sectional area) in obese older adults (Choi et al., 2016) and obese adult rodents (Kemmochi et al., 2018; Tallis et al., 2018). Part of the lower specific tension may be caused by a larger volume fraction of IMCL, that may be as high as 5% of the muscle fiber volume in obese individuals (Malenfant et al., 2001).

In addition to a decrease in force-generating capacity, fatigue resistance has also been reported to be reduced in obese people (Maffiuletti et al., 2007). Given the positive relationship between muscle fatigue resistance and oxidative capacity in motor units and single muscle fibers (Degens and Veerkamp, 1994), part of the lower fatigue resistance in skeletal muscle of obese people may be due to a reduced oxidative capacity (Crunkhorn et al., 2007; Koves et al., 2005; Shortreed et al., 2009a; Sparks et al., 2005). However, several studies in humans and rodents showed an increase in oxidative capacity with HFD (Garcia-Roves et al., 2006; Hancock et al., 2008; Iossa et al., 2002; Li et al., 2016a; Miller et al., 1984; Sadler et al., 2012), rather than a decrease. This discrepancy may be due to differences in diet duration as the effects of a HFD are time-dependent: a 4-week period of HFD resulted in little effect on the EDL oxidative capacity, but a significant increase after a 12-week period (Eshima et al., 2017). In addition, adaptations to a HFD may be muscle specific and dependent on age. For instance, in young-adult mice, it has been reported that fatigue resistance is reduced in the EDL, but not in the diaphragm and soleus muscle (Hurst et al., 2019), while in old mice 9 weeks HFD did not induce any changes in fatigue resistance in the EDL, soleus or diaphragm.

A HFD-induced shift from glucose to fatty acid metabolism may require an enhanced oxygen supply as fatty acid oxidation requires approximately 8% more oxygen than carbohydrate oxidation for each ATP generated (Silvennoinen et al., 2013). In mice, this shift in metabolism has been suggested to stimulate angiogenesis as reflected by the higher capillary density (CD) and capillary to fiber ratio (C:F) in gastrocnemius and quadriceps femoris muscles after 19 weeks HFD (Silvennoinen et al., 2013), which may be stimulated via the leptin-induced increase in VEGF-A expression (Nwadozi et al., 2019). Others, however, found no difference in the C:F or CD in the plantaris muscle of rats fed a HFD for 8 weeks (Roudier et al., 2009), and it may thus be that only after prolonged exposure to a HFD angiogenesis occurs. The effects of a HFD on the heterogeneity of capillary spacing that has an important impact on tissue oxygenation (Degens et al., 2006) is yet to be elucidated.

The majority of current available data on the effects of a HFD on skeletal muscle morphology do not consider aged animals (Bonnard et al., 2008; de Wilde et al., 2008; Eshima et al., 2017; Nwadozi et al., 2016; Silvennoinen et al., 2013). However, one study that examined the effect of an extended HFD on in vivo skeletal muscle morphology and lipid content in aged rats reported an inverse association between hind limb muscle volume and muscular lipid content

(Bollheimer et al., 2012). This observation suggests that high-fat feeding and subsequent elevated muscular lipids may contribute to age-related muscle atrophy.

The aim of the present study was to comprehensively analyze the effects of a HFD and the duration of HFD on the morphology of the soleus, EDL and diaphragm muscles in mature (20 weeks old) and early ageing (79 weeks old) mice. We hypothesized that a HFD 1) induces in all muscles an increased IMCL, and 2) that the locomotory muscles will show a *decrease* in oxidative capacity and capillarization while 3) the diaphragm shows an *increase* in oxidative capacity and capillarization, where 4) the HFD-induced changes will increase with duration of feeding and 5) be more pronounced at old age.

Materials and methods

Animal and diets

We compared the effect of HFD in the diaphragm, soleus and EDL in female CD-1 mice (Charles River, Harlan Laboratories, UK) that were 20 or 79 weeks old at the end of the experiment. The 79-week-old female mice are a model of early ageing, where survival is 50% (Navarro et al., 2002) and the muscles show morphological changes suggestive of early ageing (Messa et al., 2019), further supported by a significant declines in soleus and EDL specific tension and specific power compared to 10-week-old animals (Hill et al., 2018). In addition, the CD-1 stock is heterogeneous and therefore have greater genetic variability than many other strains of lab mice (Aldinger et al., 2009; Rice and Obrien, 1980) and as such reflect the genetic variability seen in humans.

The female CD-1 mice were housed and aged at Coventry University in cages of 8–10 individuals in 12-12h light-dark cycle at 50% relative humidity. Fifty-six 4-week-old mice and sixty 68-week-old mice were randomly allocated to either HFD or normal diet.

The 4-week-old mice were provided with normal chow (Y-CON, n=28), or a HFD for 16 weeks (YL-HFD, n=28). An additional group of mice was provided with a HFD for 8 weeks from the age of 12 weeks (YS-HFD, n = 16).

Animals used for the ageing element of the study were purchased at 9 weeks of age and provided access to a standard lab chow only during ageing. At the age of 70 weeks they either continued with regular chow (O-CON, n=30) or were given a HFD (OS-HFD, n=30) for a duration of 9 weeks.

All experimental groups provided a HFD were simultaneously provided with the standard lab chow in the form of a self-selected forage diet (Hill et al., 2019; Hurst et al., 2019). Access to each diet and water was provided *ad libitum* for all groups.

The caloric composition of the standard chow was: protein 17.5%, fat 7.4%, carbohydrate, 75.1%; gross energy 3.52 kcal.g^{-1}; metabolizable energy 2.57 kcal.g^{-1} (CRM(P) SDS/Dietex International Ltd, Whitham, UK). The caloric composition of the HFD was: protein 18.0%, fat 63.7%, carbohydrate, 18.4%; gross energy 5.2 kcal.g^{-1}; metabolizable energy 3.8 kcal.g^{-1} (Advance protocol PicoLab, Fort Worth, USA).

At the age of 20 or 79 weeks, mice were sacrificed by cervical dislocation. All experimental procedures were carried out in compliance with the local ethical review of the Coventry University under UK Home Office project license held in accordance with the Animals (Scientific procedures) Act 1986. Animals were weighed, and snout-to-anus length determined to calculate the body mass index (BMI), as body mass (kg) divided by length (cm) squared.

The removal and processing for analysis of muscle morphology of the soleus, EDL and right part of the diaphragm muscles were performed as outlined previously (Messa et al., 2019; Tallis et al., 2017b). After excision, the muscles were blotted dry, weighed, embedded in Tissue-Tek freezing medium (Leica Biosystems, Nußloch, Germany), frozen in liquid-nitrogen-cooled isopentane (Sigma-Aldrich, Steinheim, Germany) and stored at -80°C. Only one muscle per animal was collected.

Histological analysis and microscopy

Serial 10-µm thick cross-sections of the soleus, EDL and diaphragm muscles were cut with a cryostat (CM3050S; Leica, Nußloch, Germany) at -21°C and collected on Superfrost Plus microscope slides. Serial sections were stained for intramuscular cellular lipid (IMCL), myosin heavy chain (MHC), capillaries, or succinate dehydrogenase (SDH) (Messa et al., 2019).

Intramyocellular fat. Sudan Black B was utilized to stain IMCL. The Sudan Black B dye stains mainly neutral lipids (mainly triglycerides) with a blue-black tint. Briefly, air-dried sections were fixed in 10% formalin for 10 min. Sections were then washed three times for 1 min in distilled water before incubation in propylene glycol for 3 min. Sections were then incubated in the Sudan Black B solution (preheated at 60°C) for 7 min, differentiated in 85% propylene glycol for 3 min and subsequently washed three times 1 min in distilled water. Sections were cover- slipped using glycerol gelatin.

Fiber typing. Serial sections were immunohistochemically stained for type I, IIa, IIx or IIb MHC using mouse monoclonal primary antibodies BA-D5 (Supernatant; 1 $\mu g \cdot mL^{-1}$), SC-71 (Supernatant; 1 $\mu g \cdot mL^{-1}$), 6H1 (Supernatant; 10 $\mu g \cdot mL^{-1}$) and BF-F3 (Supernatant; 5 $\mu g \cdot mL^{-1}$), respectively (Development Studies Hybridoma Bank, Iowa, USA). One section was co-stained for type I, IIa and IIx MHC and a serial section for type IIb MHC.

Sections were fixed with ice-cold acetone for 15 min and then blocked for 45 min with 10% goat serum in phosphate-buffered saline (PBS) at room temperature. Following a wash with PBS, the sections were incubated with the primary antibody for 90 min in a humid chamber. The sections were subsequently washed in PBS and incubated in the dark for 60 min with Alexa Fluor 350 goat anti-mouse $IgG2_b$ (A-21140; 2 $\mu g \cdot mL^{-1}$, Invitrogen, UK) and Alexa Flour 488 goat anti-mouse IgG_1 (A-21121; 2 $\mu g \cdot mL^{-1}$, Invitrogen, UK) for type I and IIa fibers, respectively and Alexa Fluor 555 goat anti-mouse IgM (A-21426; 2 $\mu g \cdot mL^{-1}$, Invitrogen, UK) for both type IIx and IIb fibers. Sections were washed, dried and mounted using Prolong Diamond anti-fade mounting medium (Life Technologies, UK). Sections without the primary antibodies served as negative controls. Images were taken with a Carl Zeiss Axio MRc Camera (Göttingen, Germany) on a Zeiss fluorescence microscope (10-x objective).

Capillary staining. Capillaries were visualized using lectin as described previously (Ballak et al., 2016). Briefly, air-dried sections were fixed with ice-cold acetone for 15 min, and blocked with 0.1% bovine serum albumin (BSA) diluted in 2- [4- (2- hydroxyethyl)piperazin- 1- yl]ethanesulfonic acid (HEPES) for 60 min. Subsequently, the sections were treated with a peroxide solution for 30 min and incubated with biotinylated *Griffonia (Bandeira) simplicifolia* lectin (GSL I; Vector Laboratories, Peterborough, UK; 50 $\mu g \cdot mL^{-1}$ diluted in 1% BSA/HEPES) for 60 min. A 5-min wash was conducted between each step. Sections were then treated with avidin-biotinylated horseradish peroxidase (Vectastain ABC kit, Vector Laboratories, Peterborough, UK) for 60 min, washed with HEPES, and incubated with Horse Radish Peroxidase Substrate Diaminobenzidine (Vectastain DAB kit, Vector Laboratories, Peterborough, UK) for 5 min. After a wash in distilled water, the sections were mounted in glycerol gelatin (Sigma-Aldrich, Aldrich, UK).

Succinate dehydrogenase. The succinate dehydrogenase (SDH) activity was assessed according to the protocol described by Wüst et al.(2009). Sections were incubated for SDH in 37.5 mM sodium phosphate buffer (pH 7.6), 74 mM sodium succinate and 0.4 mM tetranitro blue tetrazolium in the dark at 37°C for 20 min. The reaction was stopped with 0.01 Normal

hydrochloric acid for 10 s. Then, the slides were washed with two changes of distilled water, mounted in glycerol-gelatin and stored in the dark until measurement of the staining intensity within two days. All samples were processed simultaneously in the same incubation solution, ensuring that all samples were subjected to the same conditions. Characteristic staining of EDL in an old mouse is shown in Figure 1.

Morphometry analysis

Stained sections were photographed with a digital camera (Zeiss AxioCam MRc) on a light microscope (Carl Zeiss, Göttingen, Germany; 20x objective). At least two images per muscle cross-section were taken and 245 ± 74 complete fibers were analyzed per sample.

Intramyocellular lipid. The IMCL content of individual fibers was determined using a microscope with a 20× objective and bright-field settings. Images were digitally captured using a white and black AxioCam ICMI camera (Göttingen, Germany) and analyzed with ImageJ (National Institutes of Health, USA, https://imagej.nih.gov/ij/). The fiber of interest was outlined, and the grey levels were converted to optical density (OD) using a calibration curve constructed from a series of filters of known OD. For each section, a separate calibration curve was constructed, and all images were taken at the same exposure with the same microscope settings. The OD of the Sudan Black B stain was determined in individual fibers and the background OD for each fiber was subtracted from the OD measured. The higher the net OD for the Sudan Black B stain, the higher the IMCL in the fiber.

Fiber type composition and fiber size. The fiber outlines and capillary centres were collected with a digitizing program (Program Btablet, BaLoH Software, Ooij, The Netherlands, http://www.baloh.nl) and the data analyzed with AnaTis (BaLoH Software). The fiber cross-sectional area (FCSA) was calculated for each fiber. The fiber-type composition was expressed as number percentage and as area percentage (area occupied by an individual fiber type divided by the total area occupied by all fibers).

Capillarization. The capillarization in the muscles was determined with the method of capillary domains (Degens et al., 2006; Hoofd et al., 1985) using AnaTis. Briefly, a capillary domain is defined as the area of a muscle cross-section surrounding an individual capillary delineated by equidistant boundaries from adjacent capillaries. The capillary domain provides a good estimate of the capillary oxygen supply area, even in muscles with mixed fiber type composition (Al-Shammari et al., 2014). In addition to the overall parameters of muscle capillarization, including capillary density (CD; number of capillaries per mm^2) and the

capillary to fiber ratio (C:F), this method enables the identification of the capillary supply to individual fibers even when they lack direct capillary contact. The local capillary to fiber ratio (LCFR), the sum of the fractions of the capillary domains overlapping a particular fiber, provides a continuous, rather than a discrete value of the capillary supply to a fiber and takes into consideration that a capillary supplies more than one fiber (Barnouin et al., 2017). The ratio of LCFR to the FCSA provides the capillary density for a given fiber, defined as the capillary fiber density (CFD). The radius (R) of a domain, calculated from a circle with the same surface area, provides an indication of the maximal diffusion distance from the capillary to the edge of its domain. R shows a lognormal distribution, and thus the Log_RSD (logarithmic standard deviation of the domain radius) is a measure of the heterogeneity of capillary spacing, which plays a vital role in muscle oxygenation (Degens et al., 2006; Hoofd et al., 1985).

Succinate dehydrogenase. Photomicrographs of stained sections of SDH were taken on a light microscope with a 660-nm interference filter and a white and black AxioCam ICM1 camera. All images were taken at the same exposure with the same microscope settings. Images were analyzed using ImageJ (National Institutes of Health, USA). To measure the OD of a given fiber, the outline of the fiber was drawn and the background OD subtracted. For each session, a separate calibration curve was made with filters of known OD (A_{660}). The calibration curve was used to convert the absorbance values of the SDH staining into OD values.

To assess the SDH activity (SDH-OD), the OD (A_{660}) was converted to the rate of staining and expressed as the increase in absorbance at 660 nm (A_{660}) per µm section thickness per second of incubation time ($\Delta A_{660} \cdot \mu m^{-1} \cdot s^{-1}$). The SDH-OD multiplied by the FCSA yielded the integrated SDH activity (SDH-INT in $\Delta A_{660} \cdot \mu m\ s^{-1}$):

$$\text{SDH-INT} = \text{SDH-OD} \times \text{FCSA}$$

It has been shown that the mass-specific maximal oxygen uptake (VO_{2max} in $ml \cdot kg^{-1} \cdot min^{-1}$) is proportional to SDH-OD and that the SDH-INT is linearly related to the maximum rate of oxygen uptake ($VO_{2max\ fibre}$ in $ml \cdot min^{-1}$) of the muscle fiber (van der Laarse et al., 1989).

Statistical analysis

All statistical analyses were performed using IBM SPSS version 25 (IBM SPSS Statistics for Windows, IBM Corp, Armonk, NY, USA). The Shapiro-Wilk test indicated that all data were normally distributed. The effect of diet and HFD duration were evaluated in the young-adult and old mice separately. A four-way ANOVA with the factors diet, age, muscle and fiber type

- where appropriate - applied and three-and four-way interactions were excluded. If a main effect of diet or interactions with diet were found, LSD post-hoc tests were performed to locate the differences. To assess to what extent the capillary supply to a fiber was determined by the oxidative capacity of the fiber (SDH-OD), FCSA, fiber type, muscle of origin, age and/or diet we performed a stepwise regression. Hybrid (type IIax and IIxb) were excluded from the analysis as they occurred infrequently. Statistical significance was accepted at $p < 0.05$. Data are expressed as mean ± SD.

Results

The data of the young-adult and old control muscles, and the effects of ageing have been published previously (Messa et al., 2019) and the ageing comparison is not repeated here. However, we did consider age * diet interactions, where a significant interaction indicates that the response to a HFD differs between young-adult and old mice.

In many cases, the collected muscles were not suitable for histological analysis due to damage during the preparation, freezing artefacts and/or large areas where muscle fibers were cut longitudinally; conditions that precluded adequate morphological analysis. Because of this, no data were collected for the EDL from YS-HFD mice. Nevertheless, we included them in Table 1, as they were still applicable when calculating the body and muscle masses.

Mice characteristics

In young-adult mice, an increase in body mass, BMI and soleus and EDL mass were only seen after 16 weeks of a HFD ($p \leq 0.001$; Table 1), with no significant differences from CON after 8 weeks HFD. In old mice, 9 weeks of a HFD induced an increase in body mass, BMI and soleus and EDL mass ($p \leq 0.001$; Table 1) while the muscle mass to body mass ratio was not significantly different between the HFD and CON. There were no significant diet * fiber type interactions for any of the parameters, indicating that fibers of all types responded similarly to diet. Body length did not differ significantly between the HFD and CON mice.

Intramyocellular lipid (IMCL) levels

In young-adult mice, the IMCL levels were elevated after 16 weeks HFD above CON, but not after 8 weeks HFD, in the soleus, EDL and diaphragm ($p \leq 0.006$). In the old mice 9 weeks, HFD resulted in an elevated IMCL in all three muscles ($p \leq 0.003$; Fig. 2).

Muscle fiber type composition and fiber cross-sectional areas

Fiber type composition. Figure 3 shows that the fiber type composition in the soleus (Fig. 3A & B), EDL (Fig. 3C & D) and diaphragm (Fig. 3E & F) muscles was not significantly affected by either 8-9 or 16 weeks of HFD in neither young-adult nor old mice.

Fiber cross-sectional area (FCSA). Young-adult animals on 16 weeks HFD had larger FCSAs in the soleus and diaphragm ($p \leq 0.004$), however, no significant difference in FCSA was seen between CON mice and mice 8 weeks on a HFD (Fig 4A & E). Old mice had a larger FCSA in the soleus after 9 weeks on a HFD ($p < 0.001$; Fig. 4B). In the EDL muscle, no significant differences in FCSA were observed between HFD and control groups in either young-adult or old mice (Fig. 4C & D).

Succinate dehydrogenase (SDH) activity (SDH-OD)

In young-adult mice, the mass-specific SDH activity, the SDH-OD, was higher in the soleus, EDL and diaphragm muscle from animals in the HFD than CON group, irrespective of duration of HFD ($p < 0.001$; Fig. 5A, C & E), but no significant effect of HFD was seen in the old animals (Fig. 5B, D & F). In both young-adult and old mice, the SDH-INT in the EDL was not significantly different between animals fed a HFD or CON diet in (Fig 6C & D). In young-adult mice, the SDH-INT of fibers in the soleus muscle was L-HFD > HFD > CON (Fig. 6A; $p \leq 0.033$) and in the diaphragm L-HFD > CON (Fig. 6E; $p < 0.001$). In the old mice, the HFD soleus also had a higher SDH-INT than CON (Fig. 6B; $p = 0.008$), but no significant effect of HFD was seen in the diaphragm of the old animals (Fig. 6F).

Muscle capillarization

Indices of global capillary supply. In the young animals 16 weeks, but not 8 weeks HFD, induced a significant increase in the C:F in all three muscles ($p \leq 0.006$; Table 1). In the old animals, 9 weeks HFD induced an increase in C:F in the soleus muscle only ($p = 0.006$; Table 1). There were no significant differences in the CD between control animals and animals fed for 8-9 or 16 weeks a HFD in any of the muscles from young-adult or old animals (Table 1).

There was also no significant differences in the $Log_R SD$ between CON and HFD in any of the muscles (Table 1).

Local capillary to fiber ratio (LCFR). In young animals, there was a main effect of the diet on the LCFR ($p < 0.001$, Fig. 7). However, the muscle * diet interaction ($p = 0.003$) indicated that the effect of diet differed between muscles. In the soleus muscle of young mice, the LCFR in animals on a HFD for 8 weeks was lower than CON ($p = 0.045$) and was higher in mice on 16 weeks on a HFD than CON and those on 8 weeks HFD (Fig 7A; $p \leq 0.005$). In the soleus of old mice, 9 weeks on a HFD resulted in a higher LCFR (Fig. 7B; $p < 0.001$). Post-hoc analysis revealed that in the EDL of both young and old animals the LCFR did not differ significantly between animals on a CON or HFD (Fig 7C & D). The LCFR of fibers in the diaphragm was higher in mice on a HFD for 16 weeks than CON ($p = 0.016$). There was no significant difference in diaphragm LCFR between CON and 8 weeks HFD in either young or old animals (Fig. 7E & F).

Capillary fiber density (CFD). There was no main effect of diet in either young or old animals (Fig. 8). However, the diet * muscle interaction in young animals ($p = 0.008$) was explained by a higher CFD in the diaphragm of young animals fed a HFD for 16 weeks than in control-fed or those fed a HFD for 8 weeks.

Determinants of fiber capillary supply

To assess differences between muscles, fiber types and diet in the matching of oxygen supply (LCFR) and demand (SDH-INT) of a fiber, the LCFR/SDH-INT was calculated as a measure of the supply:demand ratio. The HFD led to a decrease in the LCFR/SDH-INT of muscle fibers ($p = 0.003$), irrespective of duration of HFD, age, fiber type and muscle of origin (Fig. 9) as reflected by the absence of significant interactions between diet with age, muscle and type.

In soleus, EDL and diaphragm, the LCFR correlated positively with FCSA ($r^2 = 0.46 – 0.66$; $p < 0.001$) and this correlation did not differ significantly between CON and HFD (data not shown).

The contribution of different factors to the LCFR (capillary supply of a fiber) was assessed by performing a stepwise linear regression. The factors included in the model were FCSA, SDH-OD, muscle (soleus, EDL and diaphragm) and diet. The primary determinant of LCFR was FCSA ($r_{adj}^2 = 0.670$; $p < 0.001$), which explained most (65.3%) of the variance in LCFR.

Muscle (r_{adj}^2 = 0.783; $p < 0.001$), SDH-OD (r_{adj}^2 = 0.790; $p < 0.001$) and diet (r_{adj}^2 = 0.797; $p < 0.001$) explained an additional 12.9% of the variance in LCFR, with only a 0.7% contribution of diet.

Discussion

In the present study, we evaluated whether morphological changes induced by a high-fat diet (HFD) differed between the soleus, EDL and diaphragm and whether the adaptations differed between young-adult (20 weeks) and old mice (79 weeks). We observed that although the effect of a HFD did not differ between fiber types, the changes in muscle morphology seemed to be least pronounced in the EDL muscle. While increases in body mass and BMI, and accumulation of intramyocellular lipid (IMCL), an increase in oxidative capacity, angiogenesis and fiber hypertrophy occurred in the diaphragm and soleus muscle, they occurred sooner in old than young mice. The angiogenesis was in general proportional to the HFD-induced increase in fiber size, but signs of a developing mismatch between oxygen supply and demand were reflected by the lower ratio of capillary number: maximal oxygen consumption of a fiber (reflected by the LCFR:SDH-IT ratio) in animals on a HFD. Thus, older animals are more susceptible to HFD-induced changes in muscle morphology that may result in a mismatch between oxygen supply and demand to the working muscles.

Effects of HFD on body weight and intramyocellular lipid levels (IMCL)

The consumption of a HFD resulted in an increased BMI and muscle mass. In line with previous studies (Andrich et al., 2018; Baek et al., 2018; Eshima et al., 2017; Hegarty et al., 2002; Kaneko et al., 2011; Silvennoinen et al., 2013) this was accompanied by elevated IMCL levels of the soleus, diaphragm and EDL of our mice. This HFD-induced increase in body mass, BMI and IMCL occurred after only 9 weeks in old mice, but was only seen after 16 weeks in the young-adult mice, similar to the absence of changes in IMCL after 4 weeks, and elevated IMCL levels after 12 weeks of a HFD seen by others in young-adult mice (Eshima et al., 2017). It should be noted, however, that the BMI of the control old mice was higher than that of the young-adult mice, suggesting greater adiposity. As fatty acids are primarily stored in adipocytes and only when in excess are stored elsewhere (Koutsari et al., 2012), their larger

adiposity may cause the earlier deposition of fatty acids in the muscle of old mice. Whatever the explanation, this suggests that old mice are more susceptible to the effects of a HFD.

Muscle fiber type composition and fiber cross-sectional areas (FCSA)

Our data showed that a HFD did not induce a change in fiber type composition in any of the muscles, irrespective of age, as has been also observed by others in rodents (Shortreed et al., 2009b; Turpin et al., 2009). Eshima et al.(2017), however, reported an increased proportion of type IIx fibers concomitant with a decrease of type IIb fibers in the EDL muscle of mice on a 12-week HFD from the age of 8 weeks. The discrepancy between their study and our study may be related to the sex and strain of the mice, where we used female CD-1 mice and Eshima et al.(2017) used male C57BL/6J mice. Indeed, it has been found that 52 weeks HFD caused a decrease of type I fibers in the soleus of male, but not female mice (Denies et al., 2014). Changes in fiber type composition have regularly been given as an explanation for the obesity-induced changes in contractile function (Acevedo et al., 2017; Ciapaite et al., 2015; Kaneko et al., 2011). The absence of significant changes in fiber type composition in our study corresponds with the observation that in both the young-adult (Hurst et al., 2019; Tallis et al., 2017b) and old mice (Hill et al., 2019) there were no significant changes in the velocity of contraction at which peak power occurred or differences in fatigue resistance.

Corroborating previous observations (Bott et al., 2017; Eshima et al., 2017; Shortreed et al., 2009b; Turpin et al., 2009), we observed an increase in soleus and diaphragm FCSA of young-adult mice on a HFD for 16, but not on those on a HFD for 8 weeks. In old mice, the FCSA was already elevated in the soleus after 9 weeks HFD, indicating that the effects of HFD on soleus FCSA occurred earlier in old than young-adult mice, again supporting the notion that muscles of old mice are more susceptible to obesity or a HFD.

The hypertrophy in the postural soleus muscle may be an adaptation to the increased loading resulting from an elevated body mass (Konhilas et al., 2005; Terada et al., 2012). Indeed, in both young-adult and old mice the soleus muscle mass:body mass ratio did not change significantly after HFD. This may also explain why we did not observe a significant change in the FCSA of fibers in the EDL, which does not play a significant antigravity role. In line with this, it has been found that unloading by hindlimb suspension results in greater atrophy in the soleus than EDL muscle (Stevens et al., 2000). Nevertheless, there was no commensurate increase in absolute isometric force in the muscles of mice on a HFD (Hill et al., 2019; Hurst et al., 2019; Tallis et al., 2017b), which may be a consequence of an increased proportion of

the cytoplasmic volume occupied by IMCL. Indeed, only after 12 weeks, but not after 4 weeks on a HFD the specific tension of muscles was reduced (Eshima et al., 2017; Hurst et al., 2019; Tallis et al., 2017b) in young-adult, but surprisingly not in old muscles (Hill et al., 2019).

In the diaphragm, the FSCA increased with HFD in the young-adult mice only, but not in the old mice. It should be noted, however, that this effect on the FCSA in the diaphragm of the young-adult mice was only seen after 16 weeks on a HFD, and it is thus possible that such an increase in FCSA would also occur with longer duration of a HFD in the old mice. It is possible that the increased FCSA is compensatory hypertrophy to maintain the maximal force and power generating capacity of the diaphragm in the face of a decreased force and power generating capacity per muscle mass previously observed in the same animals after a HFD and with ageing (Hill et al., 2019; Hurst et al., 2019).

In summary, HFD did not induce changes in fiber type composition, and any increases in FCSA were muscle specific - showing no change in the EDL - occurred earlier in old than young-adult mice, and were most likely a secondary adaptation to the increased loading due to an increase in body mass, rather than a direct effect of a HFD.

Oxidative capacity

Here we showed that a HFD caused an increase in the oxidative capacity (reflected by the SDH-OD) in muscles from young-adult, but not old mice. The increase in skeletal muscle oxidative capacity with HFD has been previously reported in young-adult rodents (Eshima et al., 2017; Garcia-Roves et al., 2007; Hancock et al., 2008; Li et al., 2016b; Miller et al., 1984; Sikder et al., 2018; Thomas et al., 2014; Turner et al., 2007). Interestingly, it has been reported that the expression of enzymes in the citric acid cycle, β-oxidation and respiratory chain is comparable to standard diet after 2 weeks HFD, but similarly elevated after 8 and 16 weeks of a HFD (Sadler et al., 2012). Such HFD-induced changes in the expression of oxidative enzymes correspond to our observation of similarly elevated SDH-OD in young-adult mice on a HFD for 8 and 16 weeks. It is possible that in the young animals this elevated oxidative capacity, even in the fast EDL muscle, and associated capacity for β-oxidation may have prevented the early accumulation of IMCL in the young animals, something not seen in the old animals, where indeed IMCL accumulation already occurred after 9 weeks HFD.

The increase in SDH-OD (without an increase in IMCL) after 8 weeks of a HFD was somewhat less after 16 weeks in the diaphragm. Such a decrease may be due to lower physical activity

levels in response to a HFD (Moretto et al., 2017) that would particularly reduce the activity of the respiratory muscles. It maybe that lower physical activity levels in old than young mice (Ingram, 2000; Tallis et al., 2017a) may also underlie the absence of an increase in oxidative capacity in the muscles from old mice. Another possibility is that the increase in muscle oxidative capacity in young-adult mice is at least partly mediated by activation of peroxisome proliferator-activated receptor α (PPARα) that has been shown to induce an increased expression of genes involved in β-oxidation in neonatal cardiomyocytes (van der Lee et al., 2000). The absence of, or attenuated increase in oxidative capacity in the old mice may then be related to a reduced expression of PPARα, something observed in the heart of old mice (Bonda et al., 2017). Whatever the explanation, these data indicate that while a HFD induces an increase in muscle oxidative capacity in young-adult mice, this is not the case in old mice.

Capillarization

As discussed above, we found that a HFD induced increase in muscle oxidative capacity that in muscles from young-adult mice. This, and the reported increase in β-oxidation (Sadler et al., 2012) may reflect a shift from glucose to fatty acid metabolism. Given that per ATP 8% more oxygen is needed during fatty acid than glucose oxidation, one may argue that the muscles of young-adult mice on a HFD have a larger oxygen demand, something opposite to the pathological cardiac hypertrophy that is associated with a shift from fatty acid to glucose metabolism to overcome energy starvation (van Bilsen et al., 2004). It has therefore been suggested that to match oxygen supply with increased oxygen demand, a HFD promotes angiogenesis in addition to mitochondrial biogenesis, something reported by others (Silvennoinen et al., 2013) and in the present study as reflected by the elevated C:F and LCFR.

The absence of HFD-induced angiogenesis (no significant rise in LCFR) in the EDL and diaphragm of the old mice with no change in oxidative capacity (reflected by similar SDH-OD) appears to support the notion that HFD-induced angiogenesis may serve to ensure an adequate oxygen supply in the young-adult mice on a HFD. However, this increased demand for oxygen cannot be the sole explanation, as the increased oxidative capacity in the EDL of young-adult mice was not accompanied with angiogenesis, and in the soleus of old mice, there was angiogenesis without a significant rise in oxidative capacity. Thus, rather than a coupling between changes in oxidative capacity and capillarization, these HFD-induced changes appear to be uncoupled.

The uncoupling between changes in capillary supply and oxidative capacity of a fiber confirms our previous observation that the oxidative capacity does not determine the capillary supply to a fiber, but rather fiber size (Bosutti et al., 2015). Our data support this relationship as in all cases where an increase in fiber size occurred, there was also angiogenesis, to such an extent that the overall capillary density and the capillary density per fiber (CFD) did not differ significantly between animals on a control diet and a HFD, except for a reduction in the diaphragm from young-adult mice. The significance of fiber size and the small contribution of oxidative capacity for the capillary supply to a fiber was also reflected by a stepwise regression that showed that 67% of the variation in the capillary supply to a fiber was explicable by fiber size, with an additional 11% by muscle of origin, and only 0.7% by oxidative capacity (SDH-OD). Similar to what we have observed during ageing (Barnouin et al., 2017; Messa et al., 2019), the relationship between capillary supply with fiber size, muscle of origin and oxidative capacity was essentially unaltered by HFD (0.7% of the variation explained). This suggests that other functions of the microcirculation, such as removal of heat and waste products, and substrate delivery are more important than oxygen delivery.

Another factor that has not been considered in studies of HFD-induced obesity is the heterogeneity of capillary spacing, reflected by the logarithmic standard deviation of the capillary supply areas (Log_DSD) (Hoofd et al., 1985). Increased heterogeneity of the capillary spacing plays a role in the oxygenation of the tissue (Barnouin et al., 2017; Degens et al., 2006). The similar Log_DSD in the muscles shows that angiogenesis following a HFD does not occur at random, but rather maintains the distribution of capillaries to preserve the potential for adequate intramuscular oxygenation.

To investigate the relationship between supply and demand further we estimated the maximal oxygen demand of a fiber as the integrated SDH activity (FCSA * SDH-OD) and calculated the capillary supply (LCFR) to demand ratio (LCFR/SDH-INT) for each fiber. Following a HFD, the capillary supply to oxygen demand decreased in all muscles. This decreased ratio suggests a developing oxygen supply-demand mismatch during a HFD, similar to that seen in cardiac hypertrophy in rats (Des Tombe et al., 2002), suggesting the capillary supply becomes in deficit to oxygen capacity following a high-fat feeding. It is possible that after extended periods of HFD even capillary rarefaction occurs, something seen in muscles of obese people, that potentially could further aggravate the mismatch between oxygen supply and demand (Gomes et al., 2017).

Conclusion

The data of the present study show that the muscles of old mice are more susceptible to HFD-induced changes in morphology than young-adult mice. The adaptations are muscle specific, with an increase in fiber size in the soleus, but no change in the EDL. The increase in oxidative capacity is uncoupled from the HFD-induced angiogenesis but is explicable by increases in fiber size. It, therefore, appears that many of the HFD-induced changes in muscle morphology, except the rise in intramyocellular lipids, are a consequence of additional loading of the muscle, rather than a direct effect of a HFD. It remains to be seen how longer durations of HFD and obesity affect muscle morphology, as caspase activation will over time result in muscle wasting (Kob et al., 2015) and muscle function shows already signs of impairments (Hill et al., 2019; Hurst et al., 2019).

Disclosure The authors declare no conflict of interest.

References

Abdelmoula, A., Martin, V., Bouchant, A., Walrand, S., Lavet, C., Taillardat, M., Maffiuletti, N. A., Boisseau, N., Duche, P. and Ratel, S. (2012). Knee extension strength in obese and nonobese male adolescents. *Applied Physiology Nutrition and Metabolism* **37**, 269-275.

Acevedo, L. M., Raya, A. I., Rios, R., Aguilera-Tejero, E. and Rivero, J. L. L. (2017). Obesity-induced discrepancy between contractile and metabolic phenotypes in slow- and fast-twitch skeletal muscles of female obese Zucker rats. *Journal of Applied Physiology* **123**, 249-259.

Addison, O., Marcus, R. L., Lastayo, P. C. and Ryan, A. S. (2014). Intermuscular fat: a review of the consequences and causes. *Int J Endocrinol* **2014**, 309570.

Al-Shammari, A. A., Gaffney, E. A. and Egginton, S. (2014). Modelling capillary oxygen supply capacity in mixed muscles: Capillary domains revisited. *Journal of theoretical biology* **356**, 47-61.

Aldinger, K. A., Sokoloff, G., Rosenberg, D. M., Palmer, A. A. and Millen, K. J. (2009). Genetic Variation and Population Substructure in Outbred CD-1 Mice: Implications for Genome-Wide Association Studies. *Plos One* **4**.

Andrich, D. E., Ou, Y., Melbouci, L., Leduc-Gaudet, J. P., Auclair, N., Mercier, J., Secco, B., Tomaz, L. M., Gouspillou, G., Danialou, G. et al. (2018). Altered Lipid Metabolism Impairs Skeletal Muscle Force in Young Rats Submitted to a Short-Term High-Fat Diet. *Front Physiol* **9**, 1327.

Baek, K. W., Cha, H. J., Ock, M. S., Kim, H. S., Gim, J. A. and Park, J. J. (2018). Effects of regular-moderate exercise on high-fat diet-induced intramyocellular lipid accumulation in the soleus muscle of Sprague-Dawley rats. *Journal of Exercise Rehabilitation* **14**, 32-38.

Ballak, S. B., Buse-Pot, T., Harding, P. J., Yap, M. H., Deldicque, L., de Haan, A., Jaspers, R. T. and Degens, H. (2016). Blunted angiogenesis and hypertrophy are associated with increased fatigue resistance and unchanged aerobic capacity in old overloaded mouse muscle. *Age (Dordr)* **38**, 39.

Barnouin, Y., McPhee, J. S., Butler-Browne, G., Bosutti, A., De Vito, G., Jones, D. A., Narici, M., Behin, A., Hogrel, J. Y. and Degens, H. (2017). Coupling between skeletal muscle fiber size and capillarization is maintained during healthy aging. *Journal Of Cachexia, Sarcopenia And Muscle*.

Batsis, J. A. and Villareal, D. T. (2018). Sarcopenic obesity in older adults: aetiology, epidemiology and treatment strategies. *Nat Rev Endocrinol* **14**, 513-537.

Bollheimer, L. C., Buettner, R., Pongratz, G., Brunner-Ploss, R., Hechtl, C., Banas, M., Singler, K., Hamer, O. W., Stroszczynski, C., Sieber, C. C. et al. (2012). Sarcopenia in the aging high-fat fed rat: a pilot study for modeling sarcopenic obesity in rodents. *Biogerontology* **13**, 609-620.

Bonda, T. A., Dziemidowicz, M., Sokolowska, M., Szynaka, B., Waszkiewicz, E., Winnicka, M. M. and Kaminski, K. A. (2017). Interleukin-6 Affects Aging-Related Changes of the PPARalpha-PGC-1alpha Axis in the Myocardium. *J Interferon Cytokine Res* **37**, 513-521.

Bonen, A., Jain, S. S., Snook, L. A., Han, X. X., Yoshida, Y., Buddo, K. H., Lally, J. S., Pask, E. D., Paglialunga, S., Beaudoin, M. S. et al. (2015). Extremely rapid increase in fatty acid transport and intramyocellular lipid accumulation but markedly delayed insulin resistance after high fat feeding in rats. *Diabetologia* **58**, 2381-2391.

Bonnard, C., Durand, A., Peyrol, S., Chanseaume, E., Chauvin, M. A., Morio, B., Vidal, H. and Rieusset, J. (2008). Mitochondrial dysfunction results from oxidative stress in the skeletal muscle of diet-induced insulin-resistant mice. *Journal of Clinical Investigation* **118**, 789-800.

Bosutti, A., Egginton, S., Barnouin, Y., Ganse, B., Rittweger, J. and Degens, H. (2015). Local capillary supply in muscle is not determined by local oxidative capacity. *J Exp Biol* **218**, 3377-80.

Bott, K. N., Gittings, W., Fajardo, V. A., Baranowski, B. J., Vandenboom, R., LeBlanc, P. J., Ward, W. E. and Peters, S. J. (2017). Musculoskeletal structure and function in response to the combined effect of an obesogenic diet and age in male C57BL/6J mice. *Mol Nutr Food Res* **61**.

Cesari, M., Kritchevsky, S. B., Baumgartner, R. N., Atkinson, H. H., Penninx, B. W., Lenchik, L., Palla, S. L., Ambrosius, W. T., Tracy, R. P. and Pahor, M. (2005). Sarcopenia, obesity, and inflammation--results from the Trial of Angiotensin Converting Enzyme Inhibition and Novel Cardiovascular Risk Factors study. *Am J Clin Nutr* **82**, 428-34.

Choi, S. J., Files, D. C., Zhang, T., Wang, Z. M., Messi, M. L., Gregory, H., Stone, J., Lyles, M. F., Dhar, S., Marsh, A. P. et al. (2016). Intramyocellular Lipid and Impaired Myofiber Contraction in Normal Weight and Obese Older Adults. *Journals of Gerontology Series a-Biological Sciences and Medical Sciences* **71**, 557-564.

Ciapaite, J., van den Berg, S. A., Houten, S. M., Nicolay, K., van Dijk, K. W. and Jeneson, J. A. (2015). Fiber-type-specific sensitivities and phenotypic adaptations to dietary fat

overload differentially impact fast- versus slow-twitch muscle contractile function in C57BL/6J mice. *Journal of Nutritional Biochemistry* **26**, 155-164.

Crunkhorn, S., Dearie, F., Mantzoros, C., Gami, H., da Silva, W. S., Espinoza, D., Faucette, R., Barry, K., Bianco, A. C. and Patti, M. E. (2007). Peroxisome proliferator activator receptor gamma coactivator-1 expression is reduced in obesity - Potential pathogenic role of saturated fatty acids and p38 mitogen-activated protein kinase activation. *Journal of Biological Chemistry* **282**, 15439-15450.

de Wilde, J., Mohren, R., van den Berg, S., Boekschoten, M., Willems-Van Dijk, K., de Groot, P., Muller, M., Mariman, E. and Smit, E. (2008). Short-term high fat-feeding results in morphological and metabolic adaptations in the skeletal muscle of C57BL/6J mice. *Physiological Genomics* **32**, 360-369.

Degens, H., Deveci, D., Botto-Van Bemden, A., Hoofd, L. J. C. and Egginton, S. (2006). Maintenance of heterogeneity of capillary spacing is essential for adequate oxygenation in the soleus muscle of the growing rat. *Microcirculation* **13**, 467-476.

Degens, H. and Veerkamp, J. H. (1994). Changes in Oxidative Capacity and Fatigue Resistance in Skeletal-Muscle. *International Journal of Biochemistry* **26**, 871-878.

Denies, M. S., Johnson, J., Maliphol, A. B., Bruno, M., Kim, A., Rizvi, A., Rustici, K. and Medler, S. (2014). Diet-induced obesity alters skeletal muscle fiber types of male but not female mice. *Physiol Rep* **2**, e00204.

Des Tombe, A. L., Van Beek-Harmsen, B. J., Lee-De Groot, M. B. and Van Der Laarse, W. J. (2002). Calibrated histochemistry applied to oxygen supply and demand in hypertrophied rat myocardium. *Microsc Res Tech* **58**, 412-20.

Erskine, R. M., Tomlinson, D. J., Morse, C. I., Winwood, K., Hampson, P., Lord, J. M. and Onambele, G. L. (2017). The individual and combined effects of obesity- and ageing-induced systemic inflammation on human skeletal muscle properties. *International Journal of Obesity* **41**, 102-111.

Eshima, H., Tamura, Y., Kakehi, S., Kurebayashi, N., Murayama, T., Nakamura, K., Kakigi, R., Okada, T., Sakurai, T., Kawamori, R. et al. (2017). Long-term, but not short-term high-fat diet induces fiber composition changes and impaired contractile force in mouse fast-twitch skeletal muscle. *Physiol Rep* **5**.

Garcia-Roves, Huss, J. and Holloszy, J. O. (2006). Role of calcineurin in exercise-induced mitochondrial biogenesis. *American Journal of Physiology-Endocrinology and Metabolism* **290**, E1172-E1179.

Garcia-Roves, P., Huss, J. M., Han, D. H., Hancock, C. R., Iglesias-Gutierrez, E., Chen, M. and Holloszy, J. O. (2007). Raising plasma fatty acid concentration induces increased biogenesis of mitochondria in skeletal muscle. *Proc Natl Acad Sci U S A* **104**, 10709-13.

Garcia-Vicencio, S., Coudeyre, E., Kluka, V., Cardenoux, C., Jegu, A. G., Fourot, A. V., Ratel, S. and Martin, V. (2016). The bigger, the stronger? Insights from muscle architecture and nervous characteristics in obese adolescent girls. *International Journal of Obesity* **40**, 245-251.

Gomes, J. L., Fernandes, T., Soci, U. P., Silveira, A. C., Barretti, D. L., Negrao, C. E. and Oliveira, E. M. (2017). Obesity Downregulates MicroRNA-126 Inducing Capillary Rarefaction in Skeletal Muscle: Effects of Aerobic Exercise Training. *Oxid Med Cell Longev* **2017**, 2415246.

Hancock, C. R., Han, D. H., Chen, M., Terada, S., Yasuda, T., Wright, D. C. and Holloszy, J. O. (2008). High-fat diets cause insulin resistance despite an increase in muscle mitochondria. *Proc Natl Acad Sci U S A* **105**, 7815-20.

Hegarty, B. D., Cooney, G. J., Kraegen, E. W. and Furler, S. M. (2002). Increased efficiency of fatty acid uptake contributes to lipid accumulation in skeletal muscle of high fat-fed insulin-resistant rats. *Diabetes* **51**, 1477-1484.

Hill, James, R. S., Cox, V. M. and Tallis, J. (2018). The Effect of Increasing Age on the Concentric and Eccentric Contractile Properties of Isolated Mouse Soleus and Extensor Digitorum Longus Muscles. *J Gerontol A Biol Sci Med Sci* **73**, 579-587.

Hill, James, R. S., Cox, V. M. and Tallis, J. (2019). Does Dietary-Induced Obesity in Old Age Impair the Contractile Performance of Isolated Mouse Soleus, Extensor Digitorum Longus and Diaphragm Skeletal Muscles? *Nutrients* **11**.

Hoofd, L., Turek, Z., Kubat, K., Ringnalda, B. E. and Kazda, S. (1985). Variability of intercapillary distance estimated on histological sections of rat heart. *Adv Exp Med Biol* **191**, 239-47.

Hurst, J., James, R. S., Cox, V. M., Hill, C. and Tallis, J. (2019). Investigating a dose-response relationship between high-fat diet consumption and the contractile performance of isolated mouse soleus, EDL and diaphragm muscles. *European Journal of Applied Physiology* **119**, 213-226.

Ingram, D. K. (2000). Age-related decline in physical activity: generalization to nonhumans. *Med Sci Sports Exerc* **32**, 1623-9.

Iossa, S., Mollica, M. P., Lionetti, L., Crescenzo, R., Botta, M. and Liverini, G. (2002). Skeletal muscle oxidative capacity in rats fed high-fat diet. *Int J Obes Relat Metab Disord* **26**, 65-72.

Kaneko, S., Iida, R. H., Suga, T., Fukui, T., Morito, M. and Yamane, A. (2011). Changes in triacylglycerol-accumulated fiber type, fiber type composition, and biogenesis in the mitochondria of the soleus muscle in obese rats. *Anat Rec (Hoboken)* **294**, 1904-12.

Kemmochi, Y., Ohta, T., Motohashi, Y., Kaneshige, A., Katsumi, S., Kakimoto, K., Yasui, Y., Anagawa-Nakamura, A., Toyoda, K., Taniai-Riya, E. et al. (2018). Pathophysiological analyses of skeletal muscle in obese type 2 diabetes SDT fatty rats. *Journal of Toxicologic Pathology* **31**, 113-123.

Kob, R., Fellner, C., Bertsch, T., Wittmann, A., Mishura, D., Sieber, C. C., Fischer, B. E., Stroszczynski, C. and Bollheimer, C. L. (2015). Gender-specific differences in the development of sarcopenia in the rodent model of the ageing high-fat rat. *J Cachexia Sarcopenia Muscle* **6**, 181-91.

Konhilas, J. P., Widegren, U., Allen, D. L., Paul, A. C., Cleary, A. and Leinwand, L. A. (2005). Loaded wheel running and muscle adaptation in the mouse. *American Journal of Physiology-Heart and Circulatory Physiology* **289**, H455-H465.

Koutsari, C., Mundi, M. S., Ali, A. H. and Jensen, M. D. (2012). Storage Rates of Circulating Free Fatty Acid Into Adipose Tissue During Eating or Walking in Humans. *Diabetes* **61**, 329-338.

Koves, T. R., Li, P., An, J., Akimoto, T., Slentz, D., Ilkayeva, O., Dohm, G. L., Yan, Z., Newgard, C. B. and Muoio, D. M. (2005). Peroxisome proliferator-activated receptor-gamma co-activator 1 alpha-mediated metabolic remodeling of skeletal myocytes mimics exercise training and reverses lipid-induced mitochondrial inefficiency. *Journal of Biological Chemistry* **280**, 33588-33598.

Lee, Kim, Y., White, D. A., Kuk, J. L. and Arslanian, S. (2012). Relationships between insulin sensitivity, skeletal muscle mass and muscle quality in obese adolescent boys. *European Journal of Clinical Nutrition* **66**, 1366-1368.

Li, Chen, F., Wang, H. T., Wu, W. B., Zhang, X., Tian, C. S., Yu, H. P., Liu, R. Y., Zhu, B., Zhang, B. et al. (2016a). Non-invasive assessment of phosphate metabolism and oxidative capacity in working skeletal muscle in healthy young Chinese volunteers using P-31 Magnetic Resonance Spectroscopy. *Peerj* **4**.

Li, X., Higashida, K., Kawamura, T. and Higuchi, M. (2016b). Alternate-Day High-Fat Diet Induces an Increase in Mitochondrial Enzyme Activities and Protein Content in Rat Skeletal Muscle. *Nutrients* **8**.

Maffiuletti, N. A., Jubeau, M., Munzinger, U., Bizzini, M., Agosti, F., De Col, A., Lafortuna, C. L. and Sartorio, A. (2007). Differences in quadriceps muscle strength and fatigue between lean and obese subjects. *European Journal of Applied Physiology* **101**, 51-59.

Magnani, K. L. and Cataneo, A. J. (2007). Respiratory muscle strength in obese individuals and influence of upper-body fat distribution. *Sao Paulo Med J* **125**, 215-9.

Malenfant, P., Joanisse, D. R., Theriault, R., Goodpaster, B. H., Kelley, D. E. and Simoneau, J. A. (2001). Fat content in individual muscle fibers of lean and obese subjects. *Int J Obes Relat Metab Disord* **25**, 1316-21.

Messa, G. A. M., Piasecki, M., Hill, C., McPhee, J. S., Tallis, J. and Degens, H. (2019). Morphological alterations of mouse skeletal muscles during early ageing are muscle specific. *Experimental Gerontology*, 110684.

Miller, W. C., Bryce, G. R. and Conlee, R. K. (1984). Adaptations to a High-Fat Diet That Increase Exercise Endurance in Male-Rats. *Journal of Applied Physiology* **56**, 78-83.

Montgomery, M. K., Brown, S. H. J., Mitchell, T. W., Coster, A. C. F., Cooney, G. J. and Turner, N. (2017). Association of muscle lipidomic profile with high-fat diet-induced insulin resistance across five mouse strains. *Sci Rep* **7**, 13914.

Moretto, T. L., Benfato, I. D., de Carvalho, F. P., Barthichoto, M., Le Sueur-Maluf, L. and de Oliveira, C. A. M. (2017). The effects of calorie-matched high-fat diet consumption on spontaneous physical activity and development of obesity. *Life Sciences* **179**, 30-36.

Navarro, A., Sanchez Del Pino, M. J., Gomez, C., Peralta, J. L. and Boveris, A. (2002). Behavioral dysfunction, brain oxidative stress, and impaired mitochondrial electron transfer in aging mice. *Am J Physiol Regul Integr Comp Physiol* **282**, R985-92.

Nwadozi, E., Liu, H. Y., Roudier, E., Rullman, E., Gustafsson, T. and Haas, T. (2016). The Influence Of Obesity-Associated Metabolic Disturbance On The Profile Of Angiogenic Regulators And Capillary Number Within Skeletal Muscle. *Faseb Journal* **30**.

Nwadozi, E., Ng, A., Stromberg, A., Liu, H. Y., Olsson, K., Gustafsson, T. and Haas, T. L. (2019). Leptin is a physiological regulator of skeletal muscle angiogenesis and is locally produced by PDGFR and PDGFR expressing perivascular cells. *Angiogenesis* **22**, 103-115.

Rice and Obrien, S. J. (1980). Genetic Variance of Laboratory Outbred Swiss Mice. *Nature* **283**, 157-161.

Roudier, E., Chapados, N., Decary, S., Gineste, C., Le Bel, C., Lavoie, J. M., Bergeron, R. and Birot, O. (2009). Angiomotin p80/p130 ratio: a new indicator of exercise-induced angiogenic activity in skeletal muscles from obese and non-obese rats ? *Journal of Physiology-London* **587**, 4105-4119.

Sadler, N. C., Angel, T. E., Lewis, M. P., Pederson, L. M., Chauvigne-Hines, L. M., Wiedner, S. D., Zink, E. M., Smith, R. D. and Wright, A. T. (2012). Activity-Based Protein Profiling Reveals Mitochondrial Oxidative Enzyme Impairment and Restoration in Diet-Induced Obese Mice. *Plos One* **7**.

Shortreed, K. E., Krause, M. P., Huang, J. H., Dhanani, D., Ceddia, R. and Hawke, T. J. (2009a). Maintenance of contractile properties despite impaired skeletal muscle oxidative metabolism in diet-induced obesity. *Faseb Journal* **23**.

Shortreed, K. E., Krause, M. P., Huang, J. H., Dhanani, D., Moradi, J., Ceddia, R. B. and Hawke, T. J. (2009b). Muscle-Specific Adaptations, Impaired Oxidative Capacity and Maintenance of Contractile Function Characterize Diet-Induced Obese Mouse Skeletal Muscle. *Plos One* **4**.

Sikder, K., Shukla, S. K., Patel, N., Singh, H. and Rafiq, K. (2018). High Fat Diet Upregulates Fatty Acid Oxidation and Ketogenesis via Intervention of PPAR-gamma. *Cellular Physiology and Biochemistry* **48**, 1317-1331.

Silvennoinen, M., Rinnankoski-Tuikka, R., Vuento, M., Hulmi, J. J., Torvinen, S., Lehti, M., Kivela, R. and Kainulainen, H. (2013). High-fat feeding induces angiogenesis in skeletal muscle and activates angiogenic pathways in capillaries. *Angiogenesis* **16**, 297-307.

Sparks, L. M., Xie, H., Koza, R. A., Mynatt, R., Hulver, M. W., Bray, G. A. and Smith, S. R. (2005). A high-fat diet coordinately downregulates genes required for mitochondrial oxidative phosphorylation in skeletal muscle. *Diabetes* **54**, 1926-1933.

Stevens, L., Firinga, C., Gohlsch, B., Bastide, B., Mounier, Y. and Pette, D. (2000). Effects of unweighting and clenbuterol on myosin light and heavy chains in fast and slow muscles of rat. *Am J Physiol Cell Physiol* **279**, C1558-63.

Tallis, J., Higgins, M. F., Seebacher, F., Cox, V. M., Duncan, M. J. and James, R. S. (2017a). The effects of 8 weeks voluntary wheel running on the contractile performance of isolated locomotory (soleus) and respiratory (diaphragm) skeletal muscle during early ageing. *Journal of Experimental Biology* **220**, 3733-3741.

Tallis, J., Hill, C., James, R. S., Cox, V. M. and Seebacher, F. (2017b). The effect of obesity on the contractile performance of isolated mouse soleus, EDL, and diaphragm muscles. *J Appl Physiol (1985)* **122**, 170-181.

Tallis, J., James, R. S. and Seebacher, F. (2018). The effects of obesity on skeletal muscle contractile function. *J Exp Biol* **221**.

Terada, M., Kawano, F., Ohira, T., Nakai, N., Nishimoto, N. and Ohira, Y. (2012). Effects of Mechanical Over-Loading on the Properties of Soleus Muscle Fibers, with or without Damage, in Wild Type and Mdx Mice. *Plos One* **7**.

Thomas, M. M., Trajcevski, K. E., Coleman, S. K., Jiang, M., Di Michele, J., O'Neill, H. M., Lally, J. S., Steinberg, G. R. and Hawke, T. J. (2014). Early oxidative shifts in mouse skeletal muscle morphology with high-fat diet consumption do not lead to functional improvements. *Physiol Rep* **2**.

Tomlinson, Erskine, R. M., Winwood, K., Morse, C. I. and Onambele, G. L. (2014). The impact of obesity on skeletal muscle architecture in untrained young vs. old women. *Journal of Anatomy* **225**, 675-684.

Turner, N., Bruce, C. R., Beale, S. M., Hoehn, K. L., So, T., Rolph, M. S. and Cooney, G. J. (2007). Excess lipid availability increases mitochondrial fatty acid oxidative capacity in muscle: evidence against a role for reduced fatty acid oxidation in lipid-induced insulin resistance in rodents. *Diabetes* **56**, 2085-92.

Turpin, S. M., Ryall, J. G., Southgate, R., Darby, I., Hevener, A. L., Febbraio, M. A., Kemp, B. E., Lynch, G. S. and Watt, M. J. (2009). Examination of 'lipotoxicity' in skeletal muscle of high-fat fed and ob/ob mice. *Journal of Physiology-London* **587**, 1593-1605.

Unger, R. H., Clark, G. O., Scherer, P. E. and Orci, L. (2010). Lipid homeostasis, lipotoxicity and the metabolic syndrome. *Biochim Biophys Acta* **1801**, 209-14.

van Bilsen, M., Smeets, P. J., Gilde, A. J. and van der Vusse, G. J. (2004). Metabolic remodelling of the failing heart: the cardiac burn-out syndrome? *Cardiovasc Res* **61**, 218-26.

van der Laarse, W. J., Diegenbach, P. C. and Elzinga, G. (1989). Maximum rate of oxygen consumption and quantitative histochemistry of succinate dehydrogenase in single muscle fibres of Xenopus laevis. *J Muscle Res Cell Motil* **10**, 221-8.

van der Lee, K. A., Vork, M. M., De Vries, J. E., Willemsen, P. H., Glatz, J. F., Reneman, R. S., Van der Vusse, G. J. and Van Bilsen, M. (2000). Long-chain fatty acid-induced changes in gene expression in neonatal cardiac myocytes. *J Lipid Res* **41**, 41-7.

WHO. (2018). Obesity and overweight. Geneva, Switzerland.

Wust, R. C. I., Gibbings, S. L. and Degens, H. (2009). Fiber Capillary Supply Related to Fiber Size and Oxidative Capacity in Human and Rat Skeletal Muscle. *Oxygen Transport to Tissue Xxx* **645**, 75-80.

Zoico, E., Di Francesco, V., Guralnik, J. M., Mazzali, G., Bortolani, A., Guariento, S., Sergi, G., Bosello, O. and Zamboni, M. (2004). Physical disability and muscular strength in relation to obesity and different body composition indexes in a sample of healthy elderly women. *International Journal of Obesity* **28**, 234-241.

Table 1. Characteristics of young-adult and old female CD-1 mice fed with a control (CON) or high fat diet (HFD) and indices of overall muscle capillarisation.

	Y-CON	YS-HFD	YL-HFD	O-CON	OS-HFD
Body mass (g)	38.5 (4.9) *n*=29	40.2 (8.8) *n*=16	52.7 (12.1)[c] *n*=28	47.2 (8.8) *n*=30	58.6 (10.4)[c] *n*=30
Body length (cm)	11.3 (0.5) *n*=29	10.9 (0.4) *n*=16	11.6 (0.5) *n*=28	11.8 (0.5) *n*=30	12.4 (0.5) *n*=30
BMI ($kg \cdot m^{-2}$)	3.04 (0.32) *n*=29	3.3.8 (0.88) *n*=16	3.93 (0.79)[c,h] *n*=28	33.7 (0.44) *n*=30	3.80 (0.49)[c] *n*=30
Soleus MM (mg)	10.1 (2.7) *n*=29	10.6 (2.4) *n*=16	13.0 (4.2)[c,h] *n*=28	9.4 (2.2) *n*=30	10.9 (2.7)[c] *n*=30
Soleus MM/BM ($mg \cdot g^{-1}$)	0.26 (0.05) *n*=29	0.31 (0.08) *n*=16	0.25 (0.11) *n*=28	0.20 (0.05) *n*=30	0.19 (0.05) *n*=30
EDL MM (mg)	10.0 (0.38) *n*=29		15.4 (6.9)[c] *n*=28	10.6 (2.7) *n*=30	12.5 (2.2)[c] *n*=30
EDL MM/BM ($mg \cdot g^{-1}$)	0.28 (0.11) *n*=29		0.28 (0.16) *n*=28	0.24 (0.11) *n*=30	0.22 (0.05) *n*=30
C:F (soleus)	2.88 (0.20) *n*=6	2.90 (0.04) *n*=4	3.29 (0.23)[c] *n*=6	2.89 (0.58) *n*=5	4.01 (0.40)[c] *n*=6
C:F (EDL)	1.80 (0.29) *n*=3		1.92 (0.21)[c] *n*=3	1.73 (0.23) *n*=3	2.35 (0.41) *n*=3
C:F (diaphragm)	2.45 (0.32) *n*=7	2.35 (0.12) *n*=3	3.08 (0.61)[c] *n*=5	2.31 (0.37) *n*=5	2.27 (0.44) *n*=5
CD (soleus) (mm^{-2})	951 (106) *n*=6	909 (161) *n*=4	910 (124) *n*=6	1066 (220) *n*=5	1042 (132) *n*=6
CD (EDL) (mm^{-2})	625 (66) *n*=3		753 (155) *n*=3	1193 (214) *n*=3	1149 (92) *n*=3
CD (diaphragm) (mm^{-2})	1659 (322) *n*=7	1530 (105) *n*=3	1379 (165) *n*=5	1245 (173) *n*=5	1275 (16) *n*=5
$Log_R SD$ (soleus)	0.097 (0.009) *n*=6	0.093 (0.013) *n*=4	0.088 (0.011) *n*=6	0.093 (0.015) *n*=5	0.099 (0.007) *n*=6
$Log_R SD$ (EDL)	0.129 (0.009) *n*=3		0.119 (0.006) *n*=3	0.104 (0.014) *n*=3	0.099 (0.009) *n*=3
$Log_R SD$ (diaphragm)	0.088 (0.007) *n*=7	0.079 (0.003) *n*=3	0.093 (0.007) *n*=5	0.085 (0.003) *n*=5	0.085 (0.007) *n*=5

YL-HFD: 16 weeks HFD; YS-HFD: 8 weeks HFD; OSL-HFD: 9 weeks HFD; BM: Body mass; BMI: body mass index (body mass divided by snout-to-anus length squared); EDL: extensor digitorum longus muscle; MM/BM: muscle mass divided by BM. C:F: Capillary to fiber ratio (C:F); CD: capillary density; LogRSD: heterogeneity of capillary spacing. Values are means ± SD (n = 3-7). c different from standard diet at $p \leq 0.006$; h: different from HFD at $p \leq 0.011$

Figures

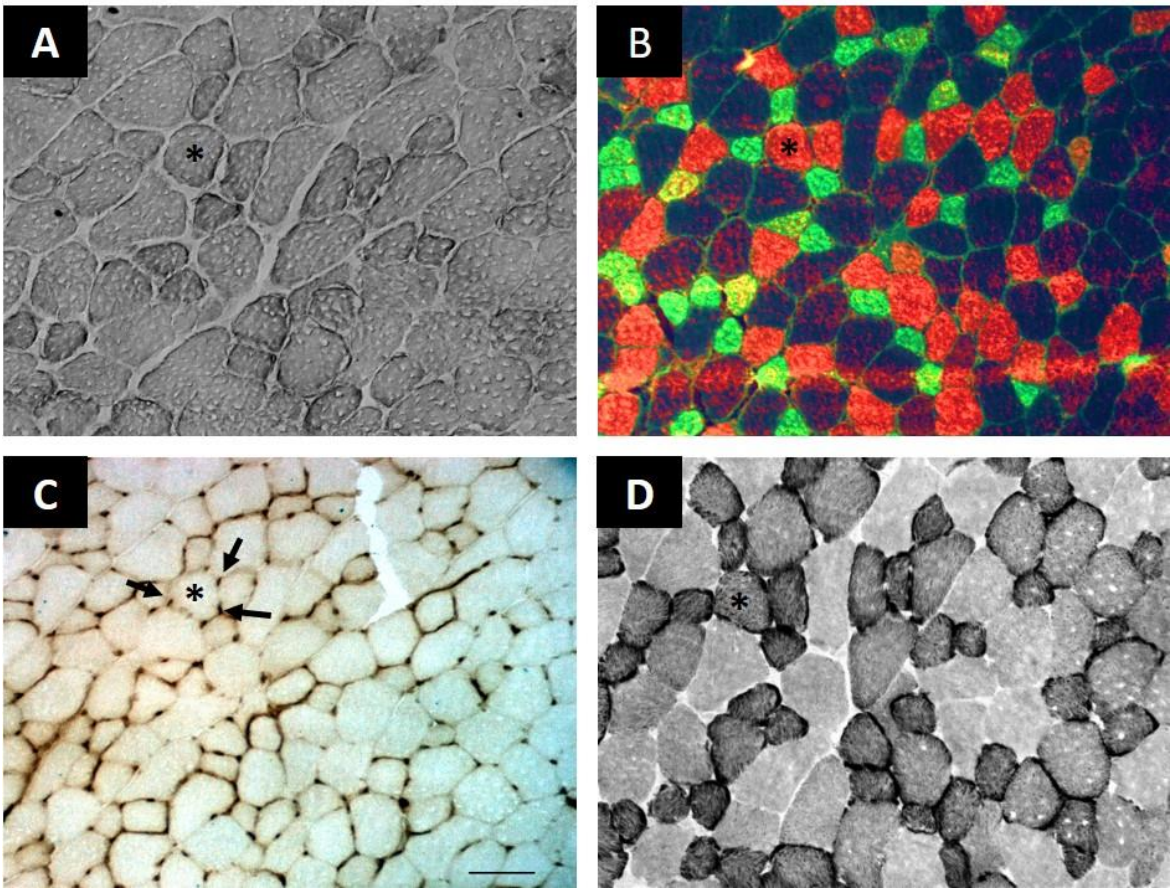

Figure 1. Serial sections of extensor digitorum lomgus from a 79-week-old mouse fed a high fat diet stained for (**A**) intramyocellular fat, (**B**) myosin heavy chain, (**C**) capillaries (arrows) and (**D**) succinate dehydrogenase (SDH) activity. *: indicates same fibre in the four panels. Green: type IIa, red: type IIx and unstained: type IIb fibers. Scale bar = 100 µm.

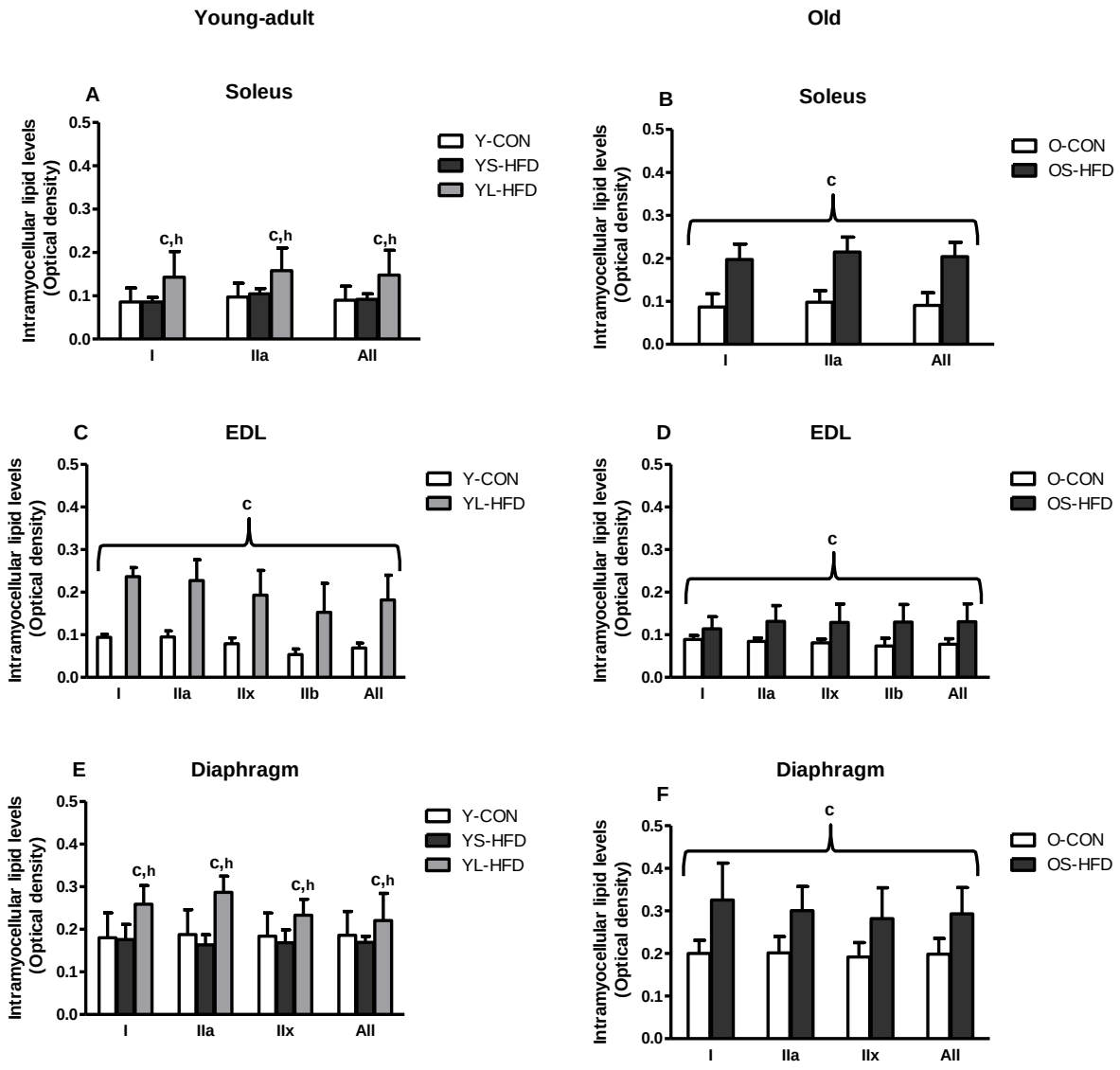

Figure 2. Intramyocellular lipids in the (A-B) soleus, **(C-D)** extensor digitorum longus (EDL) and **(E-F)** diaphragm muscles of control (CON) and 8-9 weeks of high fat diet (YS-HFD and OS-HFD, respectively) mice; L-HFD: 16 weeks HFD; left: 20-week-old mice; right: 79-week-old mice. [c] different from control; [h] different from YS-HFD at $p \leq 0.006$. Values are means ± SD (n = 3-7).

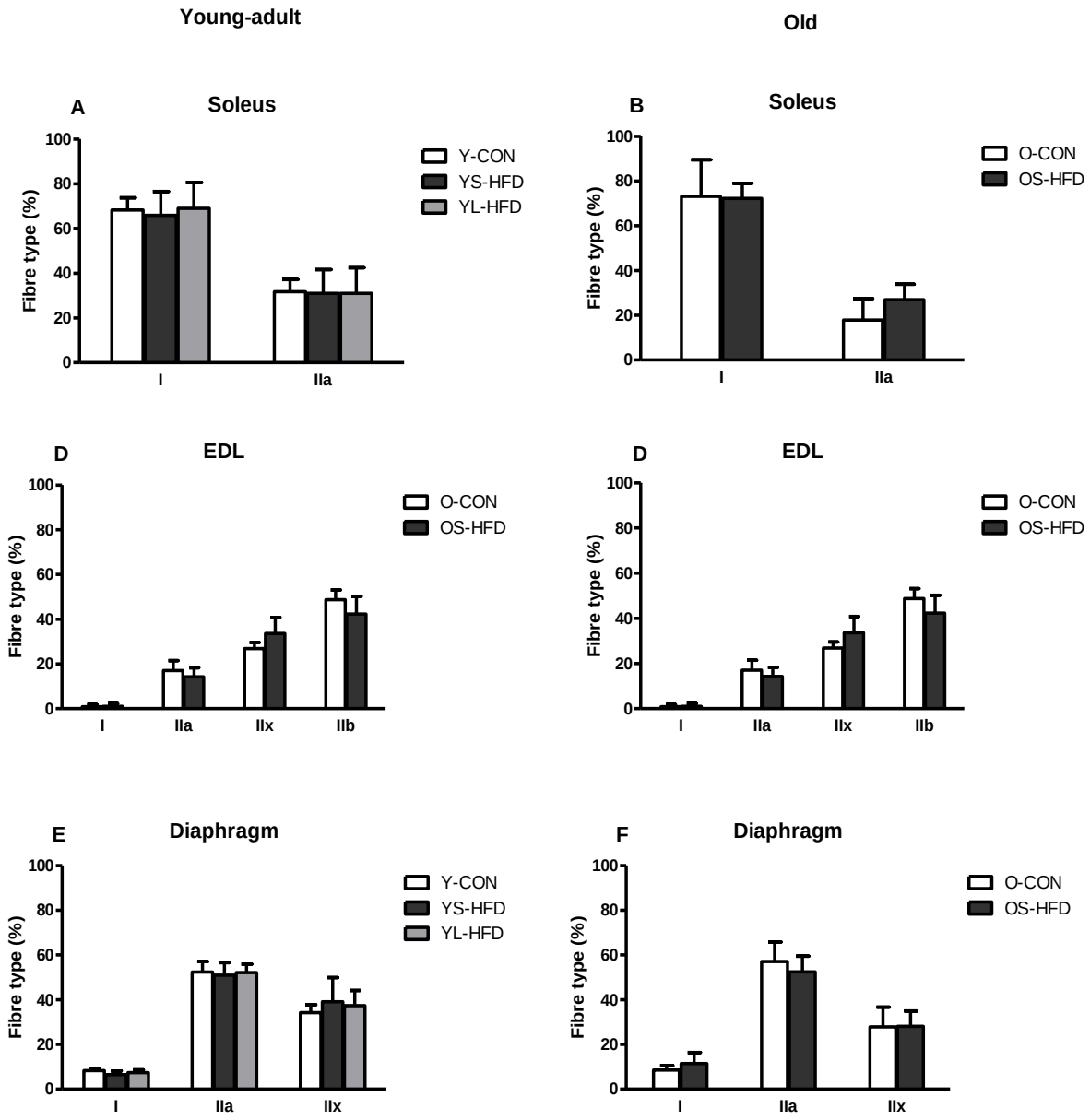

Figure 3. Fiber type composition in the (A-B) soleus, **(C-D)** extensor digitorum longus (EDL) and **(E-F)** diaphragm muscles of control (CON) and 8-9 weeks of high fat diet (YS-HFD and OS-HFD, respectively) mice; YL-HFD: 16 weeks HFD; left: 20-week-old mice; right: 79-week-old mice. Values are means ± SD (n = 3-7).

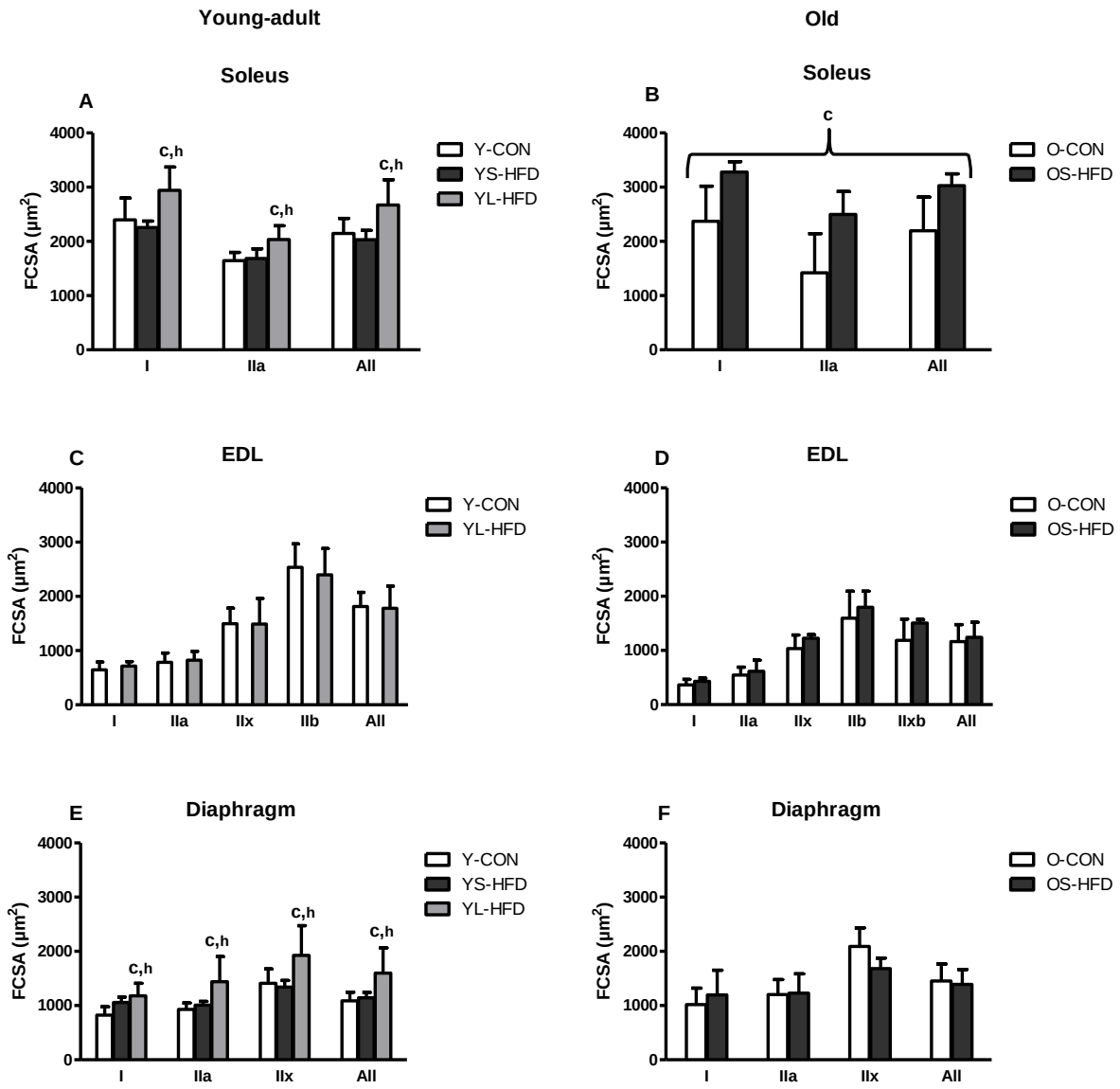

Figure 4. Fiber cross-sectional area (FCSA) in the (A-B) soleus, **(C-D)** extensor digitorum longus (EDL) and **(E-F)** diaphragm muscles of control (CON) and 8-9 weeks high fat diet (YS-HFD and OS-HFD, respectively) mice; YL-HFD: 16 weeks HFD; left: 20-week-old mice; right: 79-week-old mice. [c] different from CON; [h] different from YS-HFD at $p \leq 0.004$. Values are means ± SD (n = 3 -7).

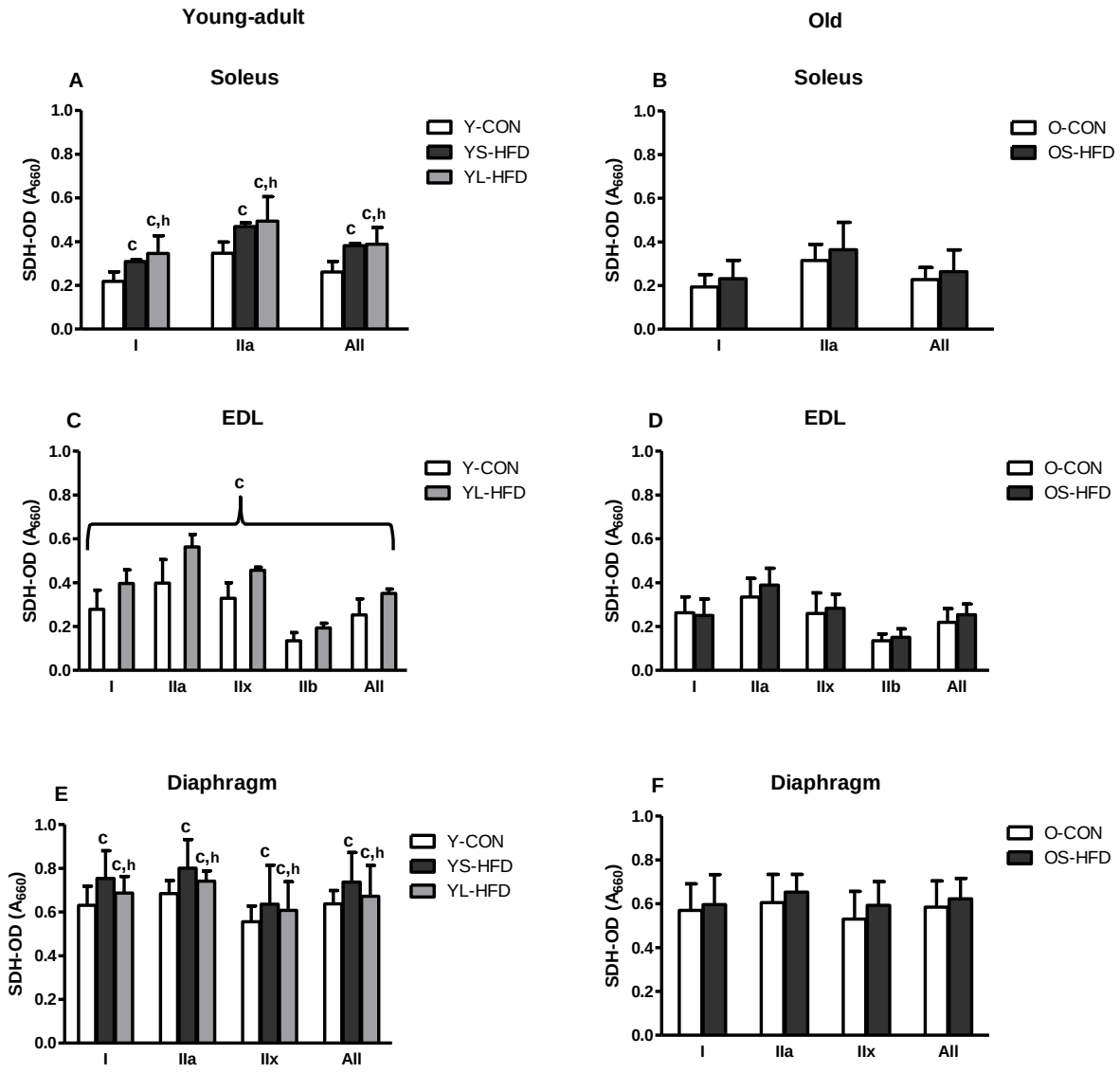

Figure 5. Succinate dehydrogenase (SDH) optical density in (A-B) soleus, **(C-D)** extensor digitorum longus (EDL) and **(E-F)** diaphragm muscles of control (CON) and 8-9 weeks high fat diet (YS-HFD and OS-HFD, respectively) mice; YL-HFD: 16 weeks HFD; left: 20-week-old mice; right: 79-week-old mice. [c] Different from CON at $p < 0.001$; [h] different from YS-HFD at $p \leq 0.025$. Values are means ± SD (n = 3-7).

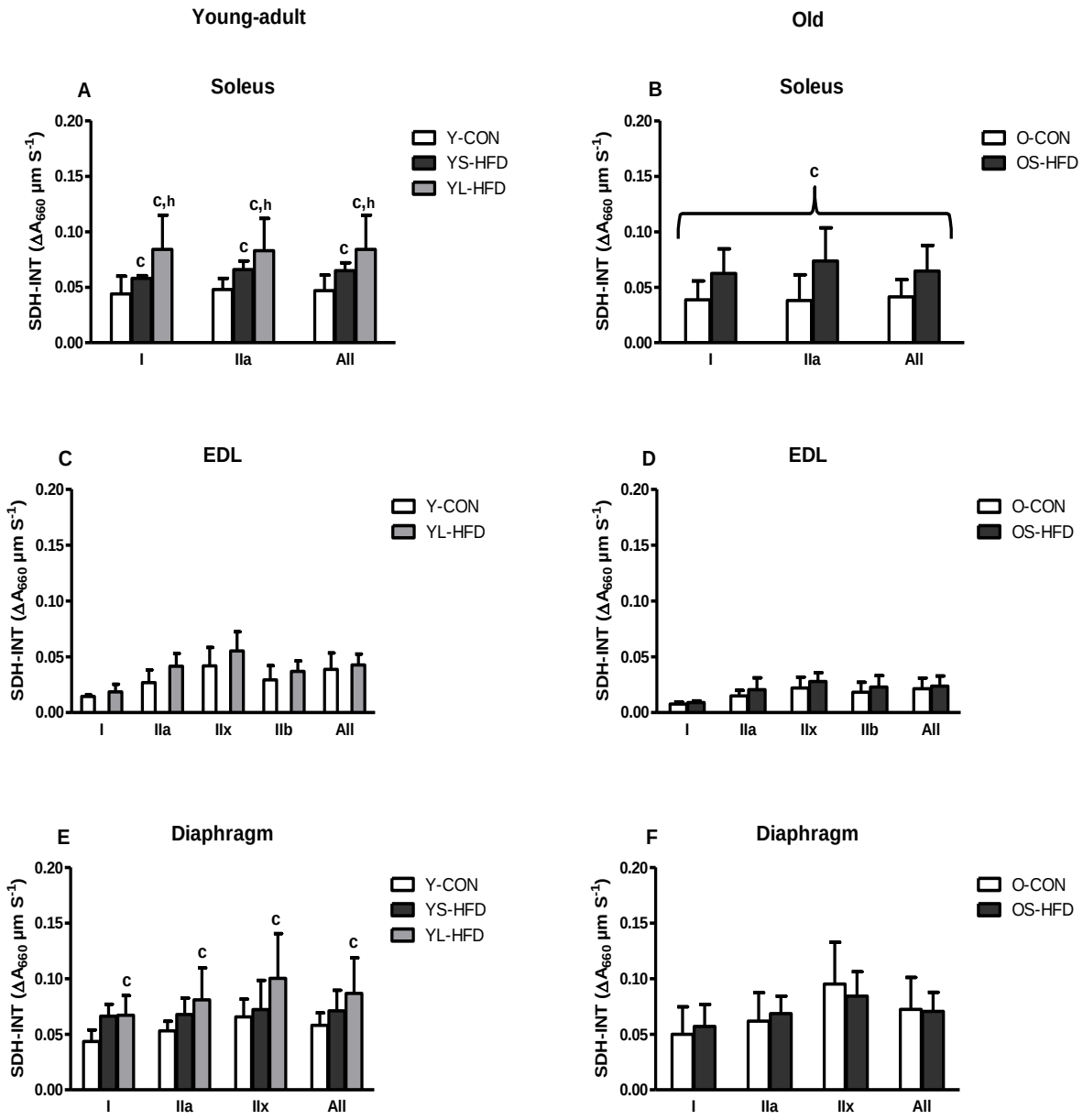

Figure 6. Integrated succinate dehydrogenase activity (SDH-INT) in (A-B) soleus, **(C-D)** extensor digitorum longus (EDL) and **(E-F)** diaphragm muscles of control (CON) and 8-9 weeks high fat diet (YS-HFD and OS-HFD, respectively) mice; YL-HFD: 16 weeks HFD; left: 20-week- and right 79-week-old mice; ; ^{h} different from YS-HFD at $p \leq 0.033$. ^{c} Different from CON at $p \leq 0.008$. Values are means ± SD (n = 3-7).

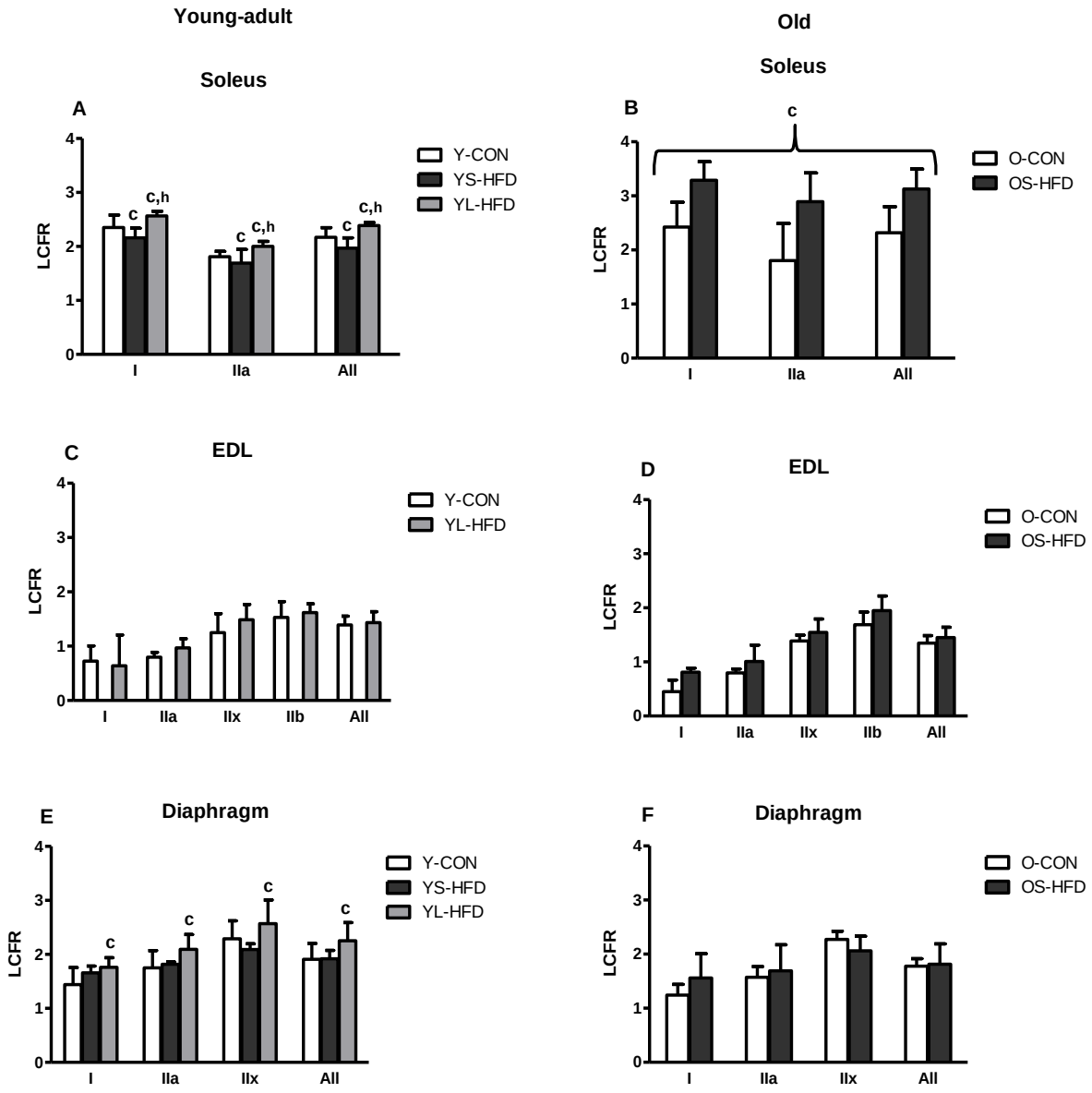

Figure 7. Local capillary to fiber ratio (LCFR) in (A-B) soleus, **(C-D)** extensor digitorum longus (EDL) and **(E-F)** diaphragm muscles of control (CON) and 8-9 weeks high fat diet (YS-HFD and OS-HFD, respectively) mice; YL-HFD: 16 weeks HFD; left: 20- and right:79-week-old mice. ^{c} different from CON at $p \leq 0.016$; ^{h} different from YS-HFD at $p = 0.045$. Values are means ± SD (n = 3-7).

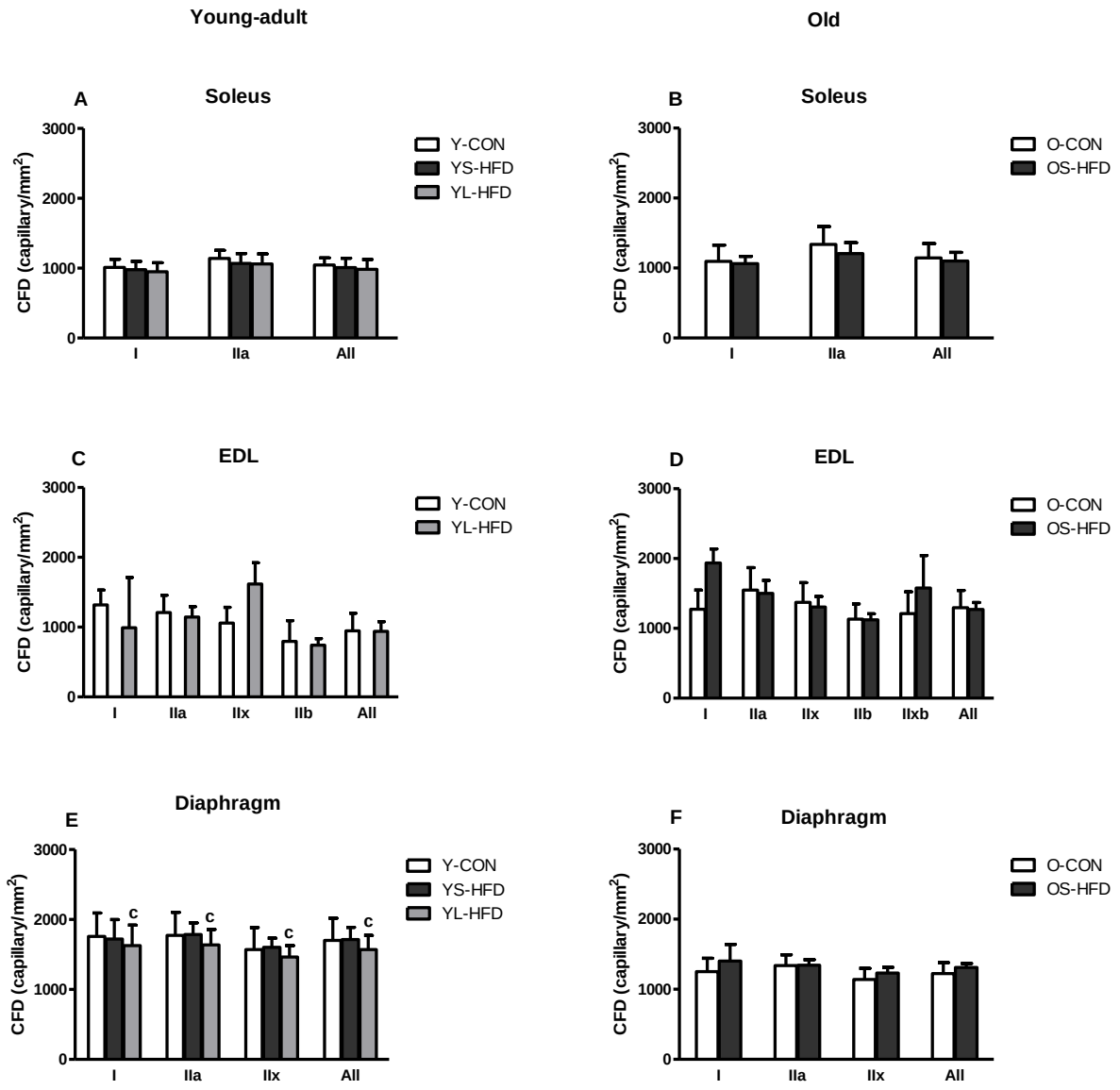

Figure 8. Capillary fiber density (CFD) in (A-B) soleus, **(C-D)** extensor digitorum longus (EDL) and **(E-F)** diaphragm muscles of control (CON) and 8-9 weeks high fat diet (YS-HFD and OS-HFD, respectively) mice; YL-HFD: 16 weeks HFD; left: 20- and right:79-week-old mice. ^{c} different from CON at $p = 0.003$. Values are means ± SD (n = 3-7).

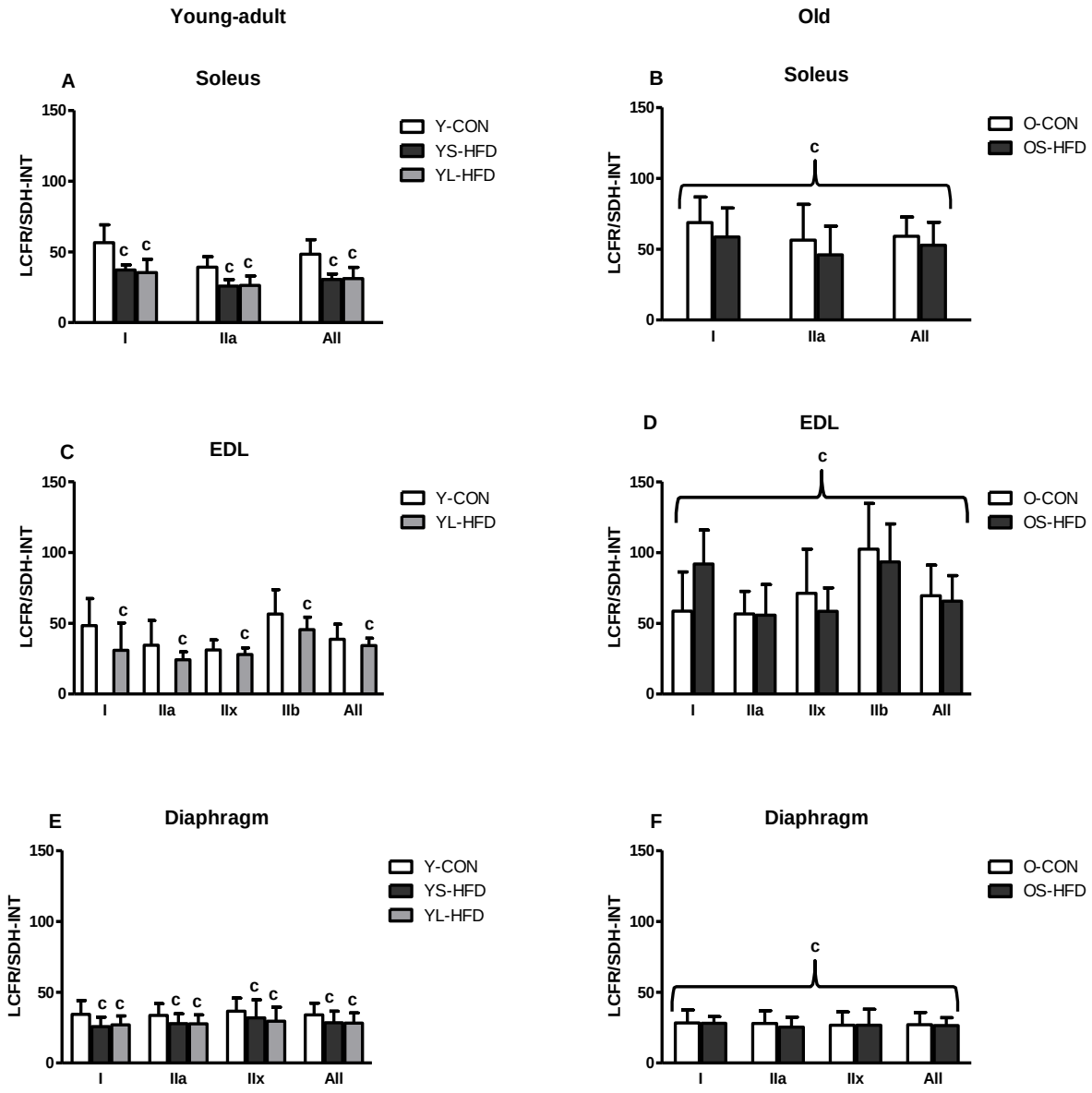

Figure 9. Local capillary to fiber ratio (LCFR):Integrated succinate dehydrogenase activity (SDH-INT) in (A-B) soleus, **(C-D)** extensor digitorum longus (EDL) and **(E-F)** diaphragm muscles of control (CON) and 8-9 weeks high fat diet (YS-HFD and OS-HFD, respectively) mice; YL-HFD: 16 weeks HFD; left: 20- and right:79-week-old mice. ^{c} main effect of diet p = 0.003. Values are means ± SD (n = 3-7).